KINETIC ANALYSIS OF PRIMATE AND ANCESTRAL ALCOHOL DEHYDROGENASES

Candace R. Myers

Submitted to the faculty of the University Graduate School
in partial fulfillment of the requirements
for the degree
Master of Science
in the Department of Biochemistry and Molecular Biology,
Indiana University

May 2012

Accepted by the Faculty of Indiana University, in partial fulfillment of the requirements for the degree of Master of Science.

Master's Thesis
Committee

_____
Thomas D. Hurley, Ph.D., Chair

_____
Mark G. Goebl, Ph.D.

_____
Amber L. Mosley, Ph.D.

For Jonathan and Jeannine Myers…

ACKNOWLEDGEMENTS

First and foremost I would like to express deep gratitude to my mentor and advisor, Dr. Tom Hurley, for his guidance and support throughout my graduate research. In addition to his academic expertise, Dr. Hurley's patience and generosity were very much appreciated and won't be forgotten. I'm grateful to have had the opportunity to work in a lab with such a great teacher.

I would also like to thank Dr. William Bosron, Dr. Sonal Sanghani, and Dr. Paresh Sanghani for their guidance during my time as a graduate student in the Biotechnology Training Program. The knowledge and skills that I acquired during this time motivated me to pursue earning a graduate degree.

Finally, I would like to thank additional members of my thesis committee, Dr. Mark Goebl and Dr. Amber Mosley, for all of their help and advice in assisting me with the completion of my Master's degree. I really appreciate the time and effort they put forth while on this committee.

ABSTRACT

Candace R. Myers

KINETIC ANALYSIS OF PRIMATE AND ANCESTRAL

ALCOHOL DEHYDROGENASES

Seven human alcohol dehydrogenase genes (which encode the primary enzymes involved in alcohol metabolism) are grouped into classes based on function and sequence identity. While the Class I ADH isoenzymes contribute significantly to ethanol metabolism in the liver, Class IV ADH isoenzymes are involved in the first-pass metabolism of ethanol.

It has been suggested that the ability to efficiently oxidize ethanol occurred late in primate evolution. Kinetic data obtained from the Class I ADH isoenzymes of marmoset and brown lemur, in addition to data from resurrected ancestral human Class IV ADH isoenzymes, supports this proposal—suggesting that two major events which occurred during primate evolution resulted in major adaptations toward ethanol metabolism.

First, while human Class IV ADH first appeared 520 million years ago, a major adaptation to ethanol occurred very recently (approximately 15 million years ago); which was caused by a single amino acid change (A294V). This change increases the catalytic efficiency of the human Class IV enzymes toward ethanol by over 79-fold. Secondly, the Class I ADH form developed 80 million years ago—when angiosperms first began to produce fleshy fruits whose sugars are fermented to ethanol by yeasts. This was followed by the duplication and divergence of distinct Class I ADH isoforms—which occurred

during mammalian radiation. This duplication event was followed by a second duplication/divergence event which occurred around or just before the emergence of prosimians (some 40 million years ago). We examined the multiple Class I isoforms from species with distinct dietary preferences (lemur and marmoset) in an effort to correlate diets rich in fermentable fruits with increased catalytic capacity toward ethanol oxidation. Our kinetic data support this hypothesis in that the species with a high content of fermentable fruit in its diet possess greater catalytic capacity toward ethanol.

Thomas D. Hurley, Ph.D., Chair

TABLE OF CONTENTS

LIST OF TABLES viii
LIST OF FIGURES ix
LIST OF ABBREVIATIONS xi
I. INTRODUCTION 1
1. Alcohol Metabolism 1
2. Alcohol Dehydrogenase 2
3. Primate Evolution and ADH Gene Duplication 7
4. Diets/Habitats of Brown Lemurs and Marmosets 9
5. Alcohol-related Diseases 10
A. Alcoholism 10
B. Alcoholic Liver Disease 11
C. Cancer 12
D. Fetal Alcohol Syndrome 12
6. Specific Aim 13
II. METHODS 24
1. Protein Purification 24
2. Activity Assay and Enzyme Kinetics 25
A. 4B Assays 27
B. 22B Assays 28
C. Sigma 2-1 Assays 29
D. Sigma 2-2 Assays 29
3. Analysis of Steady-State Kinetic Parameters 30
4. Reagents 30
5. Modeling 31
6. Determining Class I ADH Genes among Primates 31
III. RESULTS 32
1. Enzymes: 2M, 10M, 4B, and 22B 32
A. Ethanol, Propanol, Butanol, Pentanol, and Hexanol as Substrates 32
B. Cyclohexanol as a Substrate 34
C. Trans-2-hexen-1-ol as a Substrate 35
2. Enzymes: Sigma 2-1 and Sigma 2-2 37
A. Ethanol, Propanol, Butanol, Pentanol, and Hexanol as Substrates 37
B. Trans-2-hexen-1-ol as a Substrate 38
IV. DISCUSSION 47
1. Background/ Review of ADH Genes and Isoenzymes 47
2. ADH isoenzymes from Marmoset (M) and Brown Lemur (B) 49
3. Ancestral ADH Isoenzymes (Sigma 2-1 & Sigma 2-2) 52
4. Summary of Findings 54
V. CONCLUSIONS 64
REFERENCES 65
CURRICULUM VITAE

LIST OF TABLES

Table 1: K_m Constants (mM) of Human ADH Isoenzymes at pH 7.5 15
Table 2: V_{max} Constants (min^{-1}) of Human ADH Isoenzymes at pH 7.5 15
Table 3: V_{max}/K_m Values ($min^{-1}mM^{-1}$) of Human ADH Isoenzymes at pH 7.5 15
Table 4: Amino Acids Present in the Substrate Site of Human ADHs 16
Table 5: % Sequence Identity between Human and Ancestral Class IV ADH Isoenzymes 17
Table 6: % Sequence Identity between Human and Primate Class I ADH Isoenzymes 17
Table 7: K_m Constants (mM) of ADH Isoenzymes from Brown Lemur and Marmoset at pH 7.5 39
Table 8: V_{max} Constants (min^{-1}) of ADH Isoenzymes from Brown Lemur and Marmoset at pH 7.5 39
Table 9: V_{max}/K_m values ($min^{-1}mM^{-1}$) of ADH Isoenzymes from Brown Lemur and Marmoset at pH 7.5 39
Table 10: K_m Constants (mM) of Ancestral and Human ADH Isoenzymes at pH 7.5 40
Table 11: V_{max} Constants (min^{-1}) of Ancestral and Human ADH Isoenzymes at pH 7.5 40
Table 12: V_{max}/K_m Values ($min^{-1}mM^{-1}$) of Ancestral and Human ADH Isoenzymes at pH 7.5 40
Table 13: Amino Acids Present in the Substrate Site of ADHs from Marmoset and Brown Lemur 56
Table 14: Amino Acids Present in the Substrate Site of Ancestral ADHs and Human σσ-ADH 56

LIST OF FIGURES

Figure 1: Human γγ-ADH Dimer 18
Figure 2: Human αα-ADH Substrate Site 19
Figure 3: Human γγ-ADH 20
A. Side View of Substrate Site 20
B. Top View of Substrate Site 20
Figure 4: Comparison of Substrate Sites from Ancestral ADH Isoenzymes with Human σσ-ADH 57
A. Human σσ-ADH Substrate Site 57
B. Ancestral, Sigma 2-1 ADH Substrate Site 57
C. Ancestral, Sigma 2-2 ADH Substrate Site 58
Figure 5: Phylogenic Relationship of *ADH1* Paralogs 21
Figure 6: Primate Evolutionary Divergence Timeline 22
Figure 7: Primate Cladogram displaying the Nodes from which Ancestral Class IV ADHs were resurrected 23
Figure 8: Michaelis-Menten Representative Graphs of 4B-ADH from Brown Lemur with Various Aliphatic Alcohols 41
Figure 9: Michaelis-Menten Representative Graphs of 22B-ADH from Brown Lemur with Various Aliphatic Alcohols 42
Figure 10: Michaelis-Menten Representative Graphs of Brown Lemur ADHs with Cyclohexanol 43
Figure 11: Michaelis-Menten Representative Graphs of Primate and Ancestral ADHs with *Trans*-2-hexen-1-ol as a Substrate 44
Figure 12: Michaelis-Menten Representative Graphs of Ancestral, Sigma 2-1 ADH with Various Aliphatic Alcohols 45
Figure 13: Michaelis-Menten Representative Graphs of Ancestral, Sigma 2-2 ADH with Various Aliphatic Alcohols 46
Figure 14: Comparison of Position 48 in the Substrate Sites of 4B and 22B from Brown Lemur 59
A. 4B-ADH Substrate Site Displaying Position 48 59
B. 22B-ADH Substrate Site Displaying Position 48 59
Figure 15: Comparison of Position 48 in the Substrate Sites of 2M and 10M from Marmoset 60
A. 2M-ADH Substrate Site Displaying Position 48 60
B. 10M-ADH Substrate Site Displaying Position 48 60
Figure 16: Comparison of Substrate Sites of 4B from Brown Lemur and 2M from Marmoset 61
A. 4B-ADH Substrate Site 61
B. 2M-ADH Substrate Site 61
Figure 17: Comparison of Position 141 in the Substrate Sites of 22B from Brown Lemur and 10M from Marmoset 62
A. 22B-ADH Substrate Site 62
B. 10M-ADH Substrate Site 62

Figure 18: Comparison of Positions 57 and 116 in the Substrate Sites of 22B from Brown Lemur and 10M from Marmoset 63
A. 22B-ADH Substrate Site 63
B. 10M-ADH Substrate Site 63

LIST OF ABBREVIATIONS

ADH:	alcohol dehydrogenase
ALD:	alcoholic liver disease
ALDH:	aldehyde dehydrogenase
BLAST:	basal local alignment search tool
CAGE:	Cutting down, Annoyance by criticism, Guilty feeling, and Eye openers
DNA:	deoxyribonucleic acid
DTT:	dithiothreitol
ECMs:	extracellular matrices
E. coli:	*Escherichia coli*
EDTA:	ethylenediaminetetraacetic acid
FAS:	fetal alcohol syndrome
H. pylori:	*Helicobacter pylori*
HUGO:	Human Genome Organization
IPTG:	Isopropyl-β-thiogalactopyranoside
IUPUI:	Indiana University Purdue University of Indianapolis
LB:	lysogeny broth
MEOS:	microsomal ethanol-oxidizing system
NAD^+:	nicotinamide adenine dinucleotide, oxidized form
NADH:	nicotinamide adenine dinucleotide, reduced form
NCBI:	National Center for Biotechnology Information
Ni-NTA:	nickel-nitriloacetic acid
NWMs:	New World Monkeys
OD:	optical density
OWMs:	Old World Monkeys
Pdb:	protein data bank
SDS-PAGE:	sodium dodecyl sulfate polyacrylamide gel electrophoresis
Tris:	tris (hydroxymethyl) aminomethane

The standard one or three-letter abbreviations are used for symbolizing amino acids.

I. INTRODUCTION

1. Alcohol Metabolism

Ingested ethanol and intestinal ethanol of bacterial origin (from *H. pylori*) are absorbed through the digestive tract into the hepatic portal vessel—which leads to the liver (Crow & Hardman 1989). After passing through the liver, the major organ responsible for alcohol metabolism, ethanol enters the systemic circulation (Lands 1998). Any ethanol metabolized during this initial pass through the stomach, intestinal tract and liver before entering the systemic circulation is referred to as "first-pass metabolism" (Hurley *et al.* 2002).

There are three separate pathways that exist in mammalian cells for the metabolism of alcohol: (1) the two-enzyme pathway of cytosolic alcohol dehydrogenase (ADH) and mitochondrial aldehyde dehydrogenase (Shahin *et al.* 1992), (2) the MEOS—or microsomal ethanol-oxidizing system containing cytochrome P450 IIE1, and (3) catalase. The ADH-ALDH system is the primary pathway for alcohol metabolism, while the other pathways contribute significantly only under limited conditions such as chronic alcohol ingestion (Lands 1998; Lieber 1991; Inatomi *et al.* 1989).

Two distinct steps are involved in the oxidation of ethanol through the ADH-ALDH metabolic pathway. First, ADH isoenzymes catalyze the reversible oxidation of ethanol to acetaldehyde—which is then further oxidized to acetic acid by ALDH isoenzymes in the second, irreversible step. The oxidized form of nicotinamide adenine dinucleotide (NAD^+) serves as the coenzyme and electron acceptor in both steps of the ADH-ALDH pathway. The oxidation of ethanol to acetaldehyde by ADH is considered the rate-limiting step, where the equilibrium of this reaction favors the reduction of

acetaldehyde to ethanol at pH 7.0; although the reoxidation of NADH to NAD^+ can be rate-limiting under some situations (Crabb *et al.* 1983; Blacklin 1958). Alcohol dehydrogenases are the key enzymes in alcohol metabolism and make up 3% of liver soluble proteins (Edenberg & Bosron 1997). Essentially, ethanol oxidation is driven in the cell by maintaining a low ratio of products to reactants in the cytosol: the low concentration of acetaldehyde versus ethanol is maintained by the highly efficient oxidation of acetaldehyde, while NADH is re-oxidized to NAD^+ via the electron transport system in the mitochondria (Crow & Hardman 1989). Acetic acid, which is the final oxidized product, can then be further harvested for energy in mitochondria via the Krebs cycle or used for biosynthesis (Moran *et al.* 1994).

2. Alcohol Dehydrogenase

Alcohol dehydrogenases, encoded by the ADH gene family, are enzymes that metabolize various substrates: including ethanol, retinol, other aliphatic alcohols, hydroxysteroids, and lipid peroxidation products (Duester *et al.* 1999). ADH isoenzymes exist in four biological kingdoms: bacteria, yeast, plants, and animals (Branden *et al.* 1975). Human ADH isoenzymes are zinc-containing dimers consisting of two 40-kD subunits [Figure 1]. Each subunit, containing a structural zinc ion and a catalytic zinc ion, is folded into two domains: a coenzyme-binding domain and a catalytic domain. These domains are separated by a cleft containing a deep pocket—which accommodates the substrate and the nicotinamide moiety of the coenzyme. Homologous interactions between the coenzyme binding domains of each subunit link the dimers together [Figure 1] (Eklund *et al.* 1976).

Seven ADH genes have been identified in humans—*ADH1A*, *ADH1B*, *ADH1C*, *ADH4*, *ADH5*, *ADH7*, and *ADH6* (Hurley *et al.* 2002). This seven-gene cluster is found on chromosome four in humans (Edenberg 2000). All seven genes are arranges in a head-to-tail array in the order *ADH7*, *ADH1C*, *ADH1B*, *ADH1A*, *ADH6*, *ADH4*, *ADH5*. While individual genes range between 14 kilo bases (kb) and 23 kb, the spacing between them ranges from 15 kb (between Class I genes) to about 60 kb (flanking the Class I genes). The entire set of seven genes spans 365 kb (Edenberg & Bosron 1997).

ADH isoenzymes are further classified based on function and sequence identity (Duester *et al.* 1999; Edenberg 2000). There is currently some disagreement amongst investigators and the Human Genome Organization (HUGO) concerning gene nomenclature assignments. This thesis will utilize the HUGO assignments. However, the current literature can be confusing depending on which nomenclature is utilized (for review see (Duester *et al.* 1999; Hurley *et al.* 2002)). In humans, the Class I isoenzymes are encoded by genes *ADH1A*, *ADH1B*, and *ADH1C*—which yield the protein products α, β, and γ, respectively. Polymorphisms occur at the *ADH1B* and *ADH1C* loci with different distributions amongst racial populations, giving rise to the *ADH1B*1*, *ADH1B*2*, and *ADH1B*3* alleles and the *ADH1C*1* and *ADH1C*2* alleles (Hurley *et al.* 2002). The Class I enzymes and their polymeric variants can form both homo- and heterodimers (Edenberg & Bosron 1997). Class II, encoded by human *ADH4*, yields the protein product π; Class III, encoded by human *ADH5*, yields χ; and Class IV, encoded by human *ADH7* yields σ (Duester *et al.* 1999). The Class V isoenzyme, human *ADH6* has only been identified at the gene and transcriptional level—and its function remains unknown (Hoog & Ostberg 2011).

Only Class I and Class II isoenzymes contribute significantly to ethanol metabolism in the liver; where Class I isoenzymes account for approximately 70% of the total ethanol oxidizing activity at 22 mM ethanol and Class II isoenzyme accounts for 29% of ethanol oxidation at this concentration (Hurley *et al.* 2002). Although most ingested ethanol is metabolized by the liver, a small fraction is metabolized prior to ethanol's entry into systemic circulation—referred to as first pass metabolism. This includes the initial pass through the liver en route to the systemic circulation and the epithelial tissues lining the stomach, which contains high levels of the Class IV ADH (Hurley *et al.* 2002).

All three Class I ADHs are expressed in the adult liver; however, the α subunit is expressed first during development, the β subunit is expressed by mid-gestation, and the γ subunit is expressed some months after birth (Smith *et al.* 1971; Smith *et al.* 1972). Class I ADHs are also highly expressed in adrenal glands, and at lower levels in kidney, lung, skin, and other tissues (Edenberg 2000).

In general, the basic functional characteristics of Class I ADH isoenzymes are a low K_m for ethanol and a high sensitivity for inhibition by pyrazole and its four-substituted derivatives (Edenberg & Bosron 1997). As demonstrated in Tables 1, 2 and 3, Class I isoenzymes display unique substrate specificities which are derived from amino acid differences within the substrate binding site [Table 4].

While the αα isoenzyme is the least efficient Class I isoenzyme at ethanol oxidation, it is highly efficient at cyclohexanol oxidation (2800-fold and 3.5-fold higher compared to ββ and γγ, respectively) [Table 3]. The presence of alanine at position 93 instead of phenylalanine creates a more favorable environment for secondary alcohol

binding by creating more space in the substrate binding site [Table 4; Figure 2] (Gibbons & Hurley 2004).

Of all three Class I ADH isoenzymes, human ββ demonstrates the lowest K_m for ethanol [Table 1], and the lowest catalytic efficiency (V_{max}/K_m) for cyclohexanol [Table 3]. In contrast, γγ demonstrates catalytic efficiencies that increase with increasing substrate chain length among primary alcohols, as well as a 790-fold increase in V_{max}/K_m value for cyclohexanol compared to ββ [Table 3]. The amino acid substitution of threonine for serine at position 48 is essentially responsible for the kinetic differences between ββ and γγ, respectively [Table 4] (Hoog *et al.* 1992). The presence of serine at position 48 in γγ provides a larger space for bulkier substrates like cyclohexanol [Figure 3-A] (Hoog *et al.* 1992). Furthermore, this larger space accounts for the increased catalytic efficiencies of longer-chain substrates—where these substrates seem to fill the substrate binding pocket and interact more favorably with the enzyme (Light *et al.* 1992).

Figure 3-A clearly displays the inner, middle, and outer regions of the γγ substrate binding pocket. As demonstrated, positions 48 and 93 reside along the innermost part of the substrate-binding site (right-center). Moving outward (left), amino acids at positions in the middle region are visible (Val-294 and Ile-318). Continuing outward, the figure demonstrates the relative positions of Leu-57 and Leu-116 in the outer region of the binding pocket, where the surface of the enzyme is approached.

Figure 3-B displays a top view of the γγ binding site—where amino acids residing in the middle and outer regions are more visible. As demonstrated, side chains in the in the outer region (Met-306) appear closest to the viewer, whereas the middle region appears farther away (Leu-309 and Val-141).

The Class II ADH isoenzyme is expressed primarily in the liver and at lower levels in the lower gastrointestinal tract and spleen (Edenberg 2000). The ππ isoenzyme has a high K_m for ethanol and lower K_m values for medium chain alcohols [Table 1] (Bosron *et al.* 1979; Eklund *et al.* 1990). Residues in the substrate pocket of the Class II isoenzymes are longer than approximately half of the corresponding positions in comparison to Class I isoenzymes. The inner part of the substrate cleft is smaller than in Class I because Phe-93 is replaced by Tyr-93 [Table 4]—making the substrate site distinctly smaller than in Class I subunits. The narrow hydrophobic substrate binding site of ππ makes it well-designed for long aliphatic alcohols as substrates [Table 3] (Eklund *et al.* 1990).

Class III isoenzymes are ubiquitously expressed (Hur & Edenberg 1995). While the inner part of the χχ substrate-binding cleft is narrow (due to Tyr-93), the outer part is considerably wider and more polar than in the Class I and Class II isoenzymes (Eklund *et al.* 1990). This isoenzyme is probably not involved in ethanol oxidation because the K_m exceeds 2.0 M (Wagner *et al.* 1984). χχ is a long-chain ADH that also catalyzes the glutathione-dependent oxidation of formaldehyde (Koivusalo *et al.* 1989). However, its primary functional role is the metabolism of glutathione adducts (Holmquist & Vallee 1991).

Class IV is the only ADH not expressed in the liver. It is the major ethanol-active form present in the stomach; it is also found at high levels in the upper gastrointestinal tract (including esophagus, gingiva, mouth and tongue) and in the cornea and epithelial tissues (Edenberg 2000). Human σσ exhibits a high K_m for ethanol and lowered K_m values for longer chain alcohols [Table 1]. However, the catalytic efficiencies are high

with ethanol and increase as substrates increase in chain length [Table 3]. These kinetic properties arise from the presence of methionine at position 141—which relieves steric hindrance in the substrate binding site—yielding more room for larger substrates [Table 4; Figure 4-A] (Xie & Hurley 1999). In addition to being involved in the first-pass metabolism of ethanol, σσ is also the most efficient human ADH with respect to retinol oxidation (Yang *et al.* 1994).

3. Primate Evolution and ADH gene duplication

There is a single Class I ADH gene in vertebrates throughout the evolutionary tree up through primates; where gene duplication increases the number of Class I isozymic forms to two or more. The current consensus from published literature is that the first Class I ADH gene duplication occurred during mammalian radiation, followed by a second duplication that probably occurred around or just before the emergence of prosimians. Thus, at least the second duplication event of the Class I ADH genes occurred within the primate lineage (Oota *et al.* 2007). Furthermore, the absence of *ADH6* is also primate-specific. Given that *ADH1* and *ADH6* are adjacent to each other on Chromosome 4, it is possible that the duplication of *ADH1* occurred in parallel to the loss of *ADH6* in primates (Hoog & Ostberg 2011).

Recent research from the Benner group reveals the presence of four *ADH1* paralogs in the primates, *marmoset* and *macaque* [Figure 5] (Carrigan *et al.* 2012, unpublished). This finding suggests that during the course of primate evolution, multiple duplication events occurred which resulted in the formation of four Class I ADH paralogs [Figure 5]. This event is believed to have occurred prior to the divergence of Old World and New World monkeys, but after the divergence of strepsirhines (lemurs) from

haplorhines (prosimian tarsiers, NWMs, and the Catarrhini—OWMs, gibbons, orangutans, gorillas, chimpanzees, and humans). The absence of this fourth novel paralog in all remaining primates indicates that one of the paralogs was lost during the remainder of their evolution.

The basal radiation of primates occurred 63-90 million years ago (Martin 1993; Gingerich & Uhen 1994; Tavare *et al.* 2002). This was followed by the initial radiation of lemuriform primates (prosimians); which is estimated to have occurred approximately 62 million years ago in Madagascar (Yoder & Yang 2004). However, the next divergence event within the lemuriform radiation did not occur until approximately 42-43 million years ago, when prosimians and New World monkeys diverged from a common ancestor [Figure 6] (Yoder & Yang 2004).

New World monkeys (which include present-day marmosets) share a long period of common ancestry with the Catarrhini, and the divergence of these two groups occurred 35-40 million years ago [Figure 6] (Cronin & Sarich 1978). Yet, the marmoset radiation didn't begin until 7-10 million years ago (Cronin & Sarich 1978).

Due to the fact that not all primate genomes have been sequenced to date, the exact number and type of Class I ADH genes present in existing primates is unknown. However, with the use of NCBI, basic Class I ADH information for specific primate species was able to be determined. The number of Class I ADH paralogs was found to vary amongst prosimians; revealing two *ADH1*s in the bush baby, three *ADH1*s in both the mouse lemur and sifaka, and four *ADH1* paralogs in the ring-tailed lemur. While no information on brown lemur *ADH1* paralogs was obtained via NCBI, research performed for this thesis revealed the presence of at least two Class I ADHs in this species. The

marmoset (a NWM) was recently discovered to have four *ADH1* paralogs, as previously described (Carrigan *et al.* 2012, unpublished). While search results for Class I ADHs in OWMs yielded only two paralogs in the baboon (*ADH1B*-type and *ADH1C*-type), five paralogs (one of which is believed to be a pseudogene) were recently discovered in the macaque (Carrigan *et al.* 2012, unpublished). Finally, while northern gibbons, gorillas, chimpanzees, and humans all have three Class I ADHs (*ADH1A*, *ADH1B*, and *ADH1C*); orangutans appear to only have two (*ADH1A* and *ADH1C*) [Figure 5].

As demonstrated in Figure 5, humans and chimpanzees (both of which have three Class I ADH genes) diverged from a common ancestor approximately 7 million years ago (Flotte *et al.* 2010). However, the two probably had a similar diet up until about 2 million years ago (Gaulin & Konner 1977; Grine & Kay 1988); as dietary diversification is believed to have characterized human evolution over the past 2 million years (Eaton *et al.* 1997; Milton 1999; Sponheimer & Lee-Thorp 1999). Furthermore, since humans are ancestrally-derived from frugivorous primates, the preference for and excessive consumption of alcohol by modern humans may ultimately result from pre-existing sensory biases associating ethanol with nutritional reward (Dudley 2004).

4. Diets/Habitats of Brown Lemurs and Marmosets

The common brown lemur (*Eulemur fulvus*) is an arboreal primate endemic to the rainforests and dry forests of Madagascar and Mayotte (Klopfer 1970; Klopfer & Jolly 1970). These opportunistic foragers show a preference for fruits—regardless of the season—and supplement their diet with flowers and leaves (Tarnaud 2004).

The common marmoset (*Callithrix jacchus*, a small-bodied New World primate) inhabits predominantly secondary or disturbed forests, open woodlands, and savanna/dry

forest formations of northeastern and southern Brazil (Ferrari & Lopes Ferrari 1989). The common marmoset is considered among the most specialized gum-feeders (Caton *et al.* 1996; Coimbra Filho & Mittermeier 1978) and has been classified as an obligate exudativore (Garber 1992). However, when fruit is plentiful, marmosets may reduce their gum intake in favor of fruit and will also consume arthropods when available (Rylands 1984).

5. Alcohol-related Diseases

The intentional production of alcoholic beverages is currently prevalent throughout an array of human cultures world-wide. Furthermore, yeasts have been used by humans for thousands of years for fermenting food and beverages; yet fermentations were probably initiated by naturally-occurring yeasts in Neolithic times, and it is unknown when humans began to consciously add selected yeast to make beer or wine (Sicard & Legras 2011). While the moderate and/or occasional consumption of alcoholic beverages isn't generally believed to lead to any major health issues, it has been proved that excessive alcohol consumption can lead to harmful physical and mental effects.

A. Alcoholism

Alcoholism is currently recognized as a disease characterized by impaired regulation of alcohol consumption that ultimately leads to: (1) impaired control over drinking; (2) tolerance; (3) psychological dependence (craving); and (4) physical dependence (withdrawal signs upon cessation). The CAGE questions have proved useful in helping to make a diagnosis of alcoholism; where the acronym "CAGE" consists of questions which focus on Cutting down, Annoyance by criticism, Guilty feeling, and Eye-openers (Ewing 1984). This complex disease is affected by both environmental and

genetic factors. Currently the only genes that have been firmly linked to vulnerability to alcoholism are the ones encoding the alcohol and aldehyde dehydrogenases (Li 2000). Specific ADH and ALDH genes also affect risk for complications associated with alcohol abuse; including alcoholic liver disease, digestive tract cancer, heart disease, and fetal alcohol syndrome (Hurley *et al.* 2002).

B. Alcoholic Liver Disease

It is evident that the development of alcoholic liver disease (ALD) is related to the amount and duration of alcohol intake; furthermore, since not everyone exposed to equivalent amounts of alcohol develops ALD, underlying genetic factors are ultimately responsible for host susceptibility (Hurley *et al.* 2002). It is evident that oxidative stress plays an important role in the pathogenesis of ALD; where the main source of free oxygen species is cytochrome P450-dependent monooxygenase, which can be induced by ethanol (Radosavljevic *et al.* 2009).

The first and most common hepatic change caused by alcohol consumption is steatosis, or fatty liver. Hepatic fat accumulation can invoke metabolic changes that sensitize the liver to further injury (Beier & Arteel 2012). The next stage of ALD that may develop is steatohepatitis—characterized histologically by both macro- and microvesicular steatosis, and infiltration of inflammatory cells, as well as hepatocyte degeneration, ballooning, necrosis, and apoptosis (Ramaiah *et al.* 2004). Like simple steatosis, steatohepatisis is also reversible with cessation of alcohol abuse; however, the reversion can take several weeks to months, as opposed to a few days (Hill & Kugelmas 1998). The final stages of ALD include fibrosis and cirrhosis. Fibrosis is characterized by deposition of extracellular matrices, or ECMs (Schuppan *et al.* 2001). If alcohol

intake persists past fibrosis, cirrhosis can develop—which consists of hepatic scarring (as with fibrosis, but more extensive), altered liver parenchyma with septae and nodule formation, and distorted hepatic blood flow (Friedman 2008; Kim *et al.* 2002). Upon cirrhosis development, death will probably occur without a liver transplant (Kim *et al.* 2002).

C. Cancer

An increased risk for upper aerodigestive tract (oral cavity, pharynx, larynx, and esophagus), stomach, and colorectal cancers are associated with high levels of chronic alcohol consumption. In essence, acetaldehyde causes point mutations in DNA and induces sister chromatid exchanges and abberations; thus having direct mutagenic and carcinogenic effects (Dellarco 1988).

Many studies have shown that the *ALDH2*2* allele is associated with an increased risk of ethanol-associated digestive tract cancers; while some studies have found an association of *ADH1B*1* and *ADH1C*2* with an increased risk for oropharyngeal cancer (Yokoyama *et al.* 1998; Olshan *et al.* 2001).

D. Fetal Alcohol Syndrome

Fetal alcohol syndrome (FAS) is a pattern of birth defects caused by maternal ethanol consumption during pregnancy. FAS is recognized by growth deficiency, a characteristic set of craniofacial features, and neurodevelopmental abnormalities leading to cognitive and behavioral deficits (Stratton *et al.* 1996). While it is evident that alcohol is an environmental teratogen, it is unclear which principal agent (ethanol itself or acetaldehyde) triggers the developmental abnormalities in the brain during gestation (Hurley *et al.* 2002).

However, it is known that retinol and ethanol are competitive substrates for oxidation by ADH to retinal and acetaldehyde, respectively; furthermore, retinoic acid—derived from vitamin A (retinol)—is essential for controlling the normal patterns of development of tissues and organs (Deltour *et al.* 1999).

6. Specific Aims

The overlying hypothesis of this thesis is that the evolution of ethanol oxidizing capability amongst primates is driven by dietary factors and that alcohol dehydrogenase isoenzymes evolved in a manner to increase their catalytic efficiency toward small substrates like ethanol due to increased prevalence of fermented alcohols present in ripened fruit. Research for this thesis focused on the enzymatic properties of multiple Class I ADH isoenzymes from two modern-day primates with distinct dietary habits, in addition to the enzymatic properties of different Class IV ADH isoenzymes resurrected from human ancestors. The protein sequences from primate ADH isoenzymes were compared to human Class I isoenzymes [Table 5], while protein sequences from ancestral ADH isoenzymes were compared to the human Class IV isoenzyme [Table 6] utilizing the BLAST tool. Next, enzymatic properties obtained via kinetic assays and structural analysis were compared to ADH isoenzymes of modern-day humans in order to determine the efficiency of alcohol metabolism—especially ethanol metabolism—among respective species. This information was ultimately used in order to determine when and why ADH isoenzymes duplicated and diverged during the evolution of primates.

We chose to examine multiple Class I ADH isoforms from primate species with distinct dietary preferences (brown lemur and marmoset) in an effort to correlate diets rich in fermentable fruits with increased catalytic capacity toward ethanol oxidation. The

ancestral Class IV ADH isoforms were selected from two nodes common to humans, which are known to possess isoenzymes containing alanine at position 294 [Figure 7]. Since modern humans possess a Class IV isoform containing valine at this position, Sigma 2-1 and Sigma 2-2 were chosen in an effort to determine the effect/magnitude of change in catalytic capacity toward ethanol oxidation caused by this single amino acid exchange—which is believed to have occurred approximately 15 million years ago in primate evolution – and may be the major contributor to the increased capacity of human Class IV ADH to oxidize ethanol.

Table 1: K_m Constants (mM) of Human ADH Isoenzymes at pH 7.5

	Human ADH isoenzymes→	αα[1,2]	ββ[1,2]	γγ[1]	σσ[3]	χχ[4]	ππ[4]
SUBSTRATES	Ethanol	6.1	0.05	0.33	28	*	120
	Propanol	0.6	0.019	~	1.4	~	~
	Butanol	0.032	0.012	0.04	0.79	~	~
	Pentanol	0.014	0.019	0.02	0.28	22	0.09
	Hexanol	~	0.022	~	0.13	8.2	~
	Trans-2-hexen-1-ol	~	~	~	0.018	~	~
	Cyclohexanol	0.012	3.9	0.063	~	#	210

Table 2: V_{max} Constants (min^{-1}) of Human ADH Isoenzymes at pH 7.5

	Human ADH isoenzymes→	αα[1,2]	ββ[1,2]	γγ[1]	σσ[3]	χχ[4]	ππ[4]
SUBSTRATES	Ethanol	16	4.0	49	1,800	*	470
	Propanol	22	3.0	~	1,000	~	~
	Butanol	20	2.9	74	2,100	~	~
	Pentanol	15	3.6	68	960	240	480
	Hexanol	~	4.4	~	1,200	130	~
	Trans-2-hexen-1-ol	~	~	~	2,200	~	~
	Cyclohexanol	25	3.0	38	~	~	35

Table 3: V_{max}/K_m Values ($min^{-1}mM^{-1}$) of Human ADH Isoenzymes at pH 7.5

	Human ADH isoenzymes→	αα[1,2]	ββ[1,2]	γγ[1]	σσ[3]	χχ[4]	ππ[4]
SUBSTRATES	Ethanol	2.7	80	150	65	*	4
	Propanol	36	160	~	570	~	~
	Butanol	640	240	1,800	2,600	~	~
	Pentanol	1,100	190	3,400	3,400	11	5,300
	Hexanol	~	200	~	9,000	16	~
	Trans-2-hexen-1-ol	~	~	~	120,000	~	~
	Cyclohexanol	2,100	0.76	600	~	#	0.2

(All data was rounded to 2 significant figures.)

1. (Stone *et al.* 1989)
2. (Hurley & Bosron 1992)
3. (Kedishvili *et al.* 1995)
4. (Eklund *et al.* 1987); measured at pH 10.0

= No activity
* = No saturation
~ = Not determined

Table 4: Amino Acids Present in the Substrate Site of Human ADHs

REGION	Position	Human Class I			II	III	IV
		αα	ββ	γγ	ππ	χχ	σσ
INNER	48	Thr	Thr	Ser	Thr	Thr	Thr
	93	Ala	Phe	Phe	Tyr	Tyr	Phe
MIDDLE	141	Leu	Leu	Val	Phe	Met	Met
	294	Val	Val	Val	Val	Val	Val
	309	Leu	Leu	Leu	Ile	Val	Phe
	318	Ile	Val	Ile	Phe	Ala	Val
OUTER	57	Met	Leu	Leu	Phe	Asp	Met
	116	Val	Leu	Leu	Asn	Val	Ile
	306	Met	Met	Met	Glu	Phe	Met

Table 5: % Sequence Identity between Human and Ancestral Class IV ADH Isoenzymes

	Human σσ	Sigma 2-1	Sigma 2-2
Human σσ		97%	99%
Sigma 2-1	97%		98%
Sigma 2-2	99%	98%	

Table 6: % Sequence Identity between Human and Primate Class I ADH Isoenzymes

	ADH1A	*ADH1B*	*ADH1C*	2M	10M	4B	22B
ADH1A		94%	93%	90%	90%	87%	86%
ADH1B	94%		94%	93%	91%	86%	85%
ADH1C	93%	94%		93%	93%	87%	87%
2M	90%	93%	93%		90%	86%	83%
10M	90%	91%	93%	90%		87%	85%
4B	87%	86%	87%	86%	87%		89%
22B	86%	85%	87%	83%	85%	89%	

Figure 1: Human γγ-ADH Dimer

Figure 1

-Ribbons diagram of human γγ -ADH with different colors representing different subunits (teal and green).
-Bound coenzyme molecules are displayed in magenta.
-Generated with PyMOL.

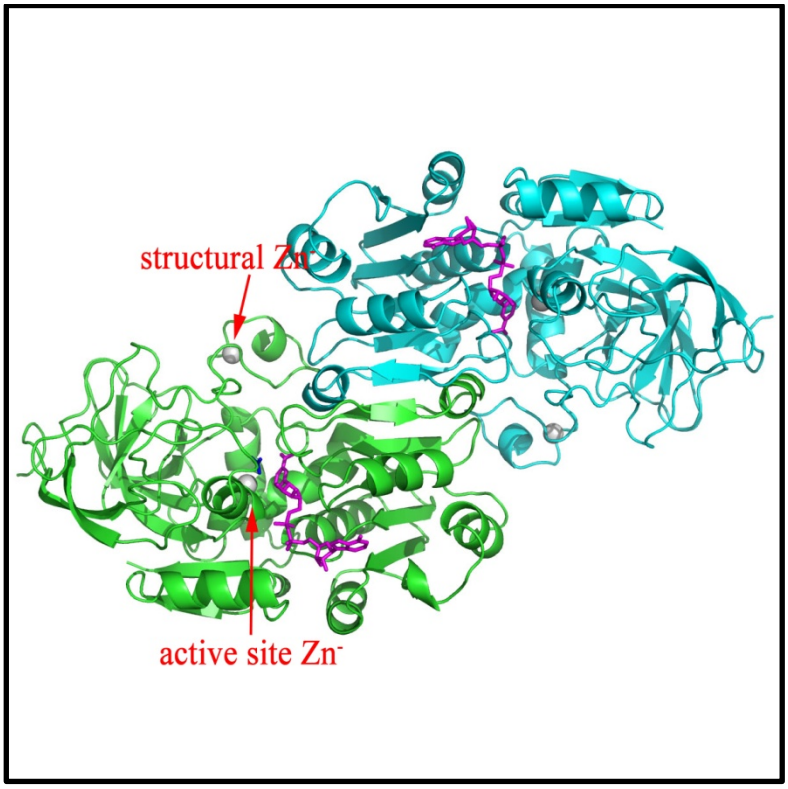

Figure 2: Human αα-ADH Substrate Site

Figure 2

-Side view of human αα-ADH displaying Ala-93 in the Inner Region, Val-294 in the Middle Region, and Val-116 in the Outer Region of the substrate binding site.
-The Phe→Ala substitution at position 93 results in extra space in the substrate binding site compared to ββ-ADH and γγ-ADH.
-Generated with PyMOL.

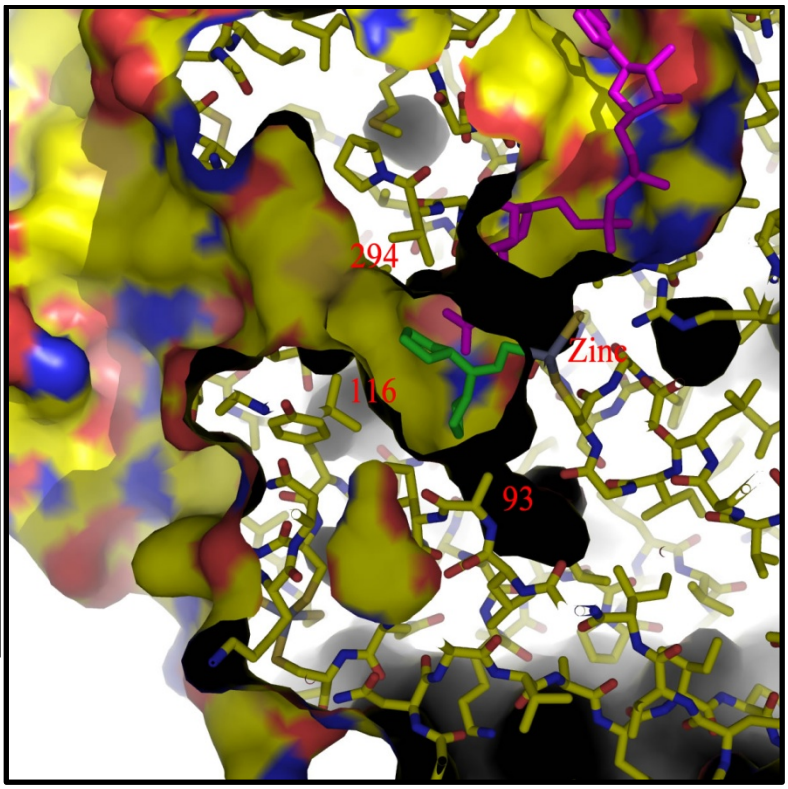

Figure 3: Human γγ-ADH

A. Side View of Substrate Site

Figure 3-A

-Side view of humaηγγ-ADH displaying Ser-48 and Phe-93 in the Inner Region, Val-294 and Ile-318 in the Middle Region, and Leu-57 and Leu-116 in the Outer Region of the substrate binding site.
-Generated with PyMOL.

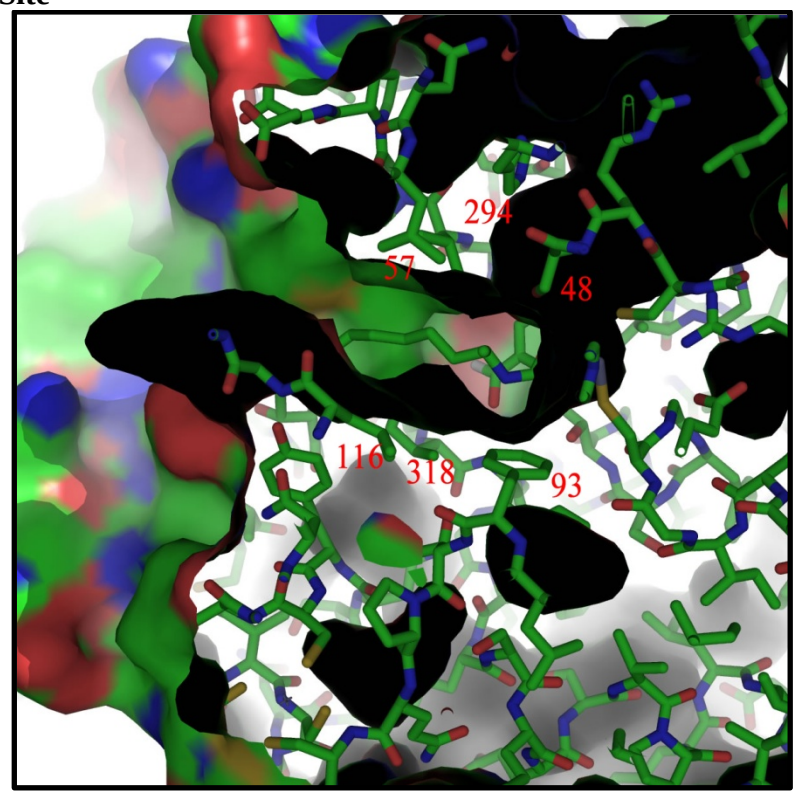

B. Top View of Substrate Site

Figure 3-B

-Top view of huma γγ-ADH displaying Phe-140, Val-141 and Leu-309 in the Middle Region, and Met-306 in the Outer Region of the substrate binding site.
-Generated with PyMOL.

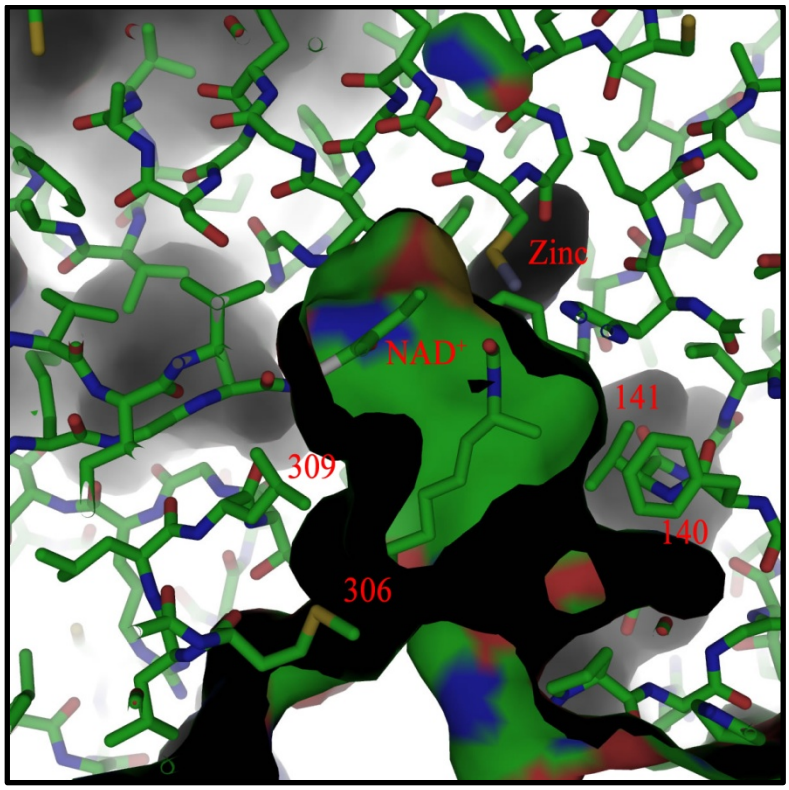

Figure 5: Phylogenetic Relationship of *ADH1* Paralogs[1]

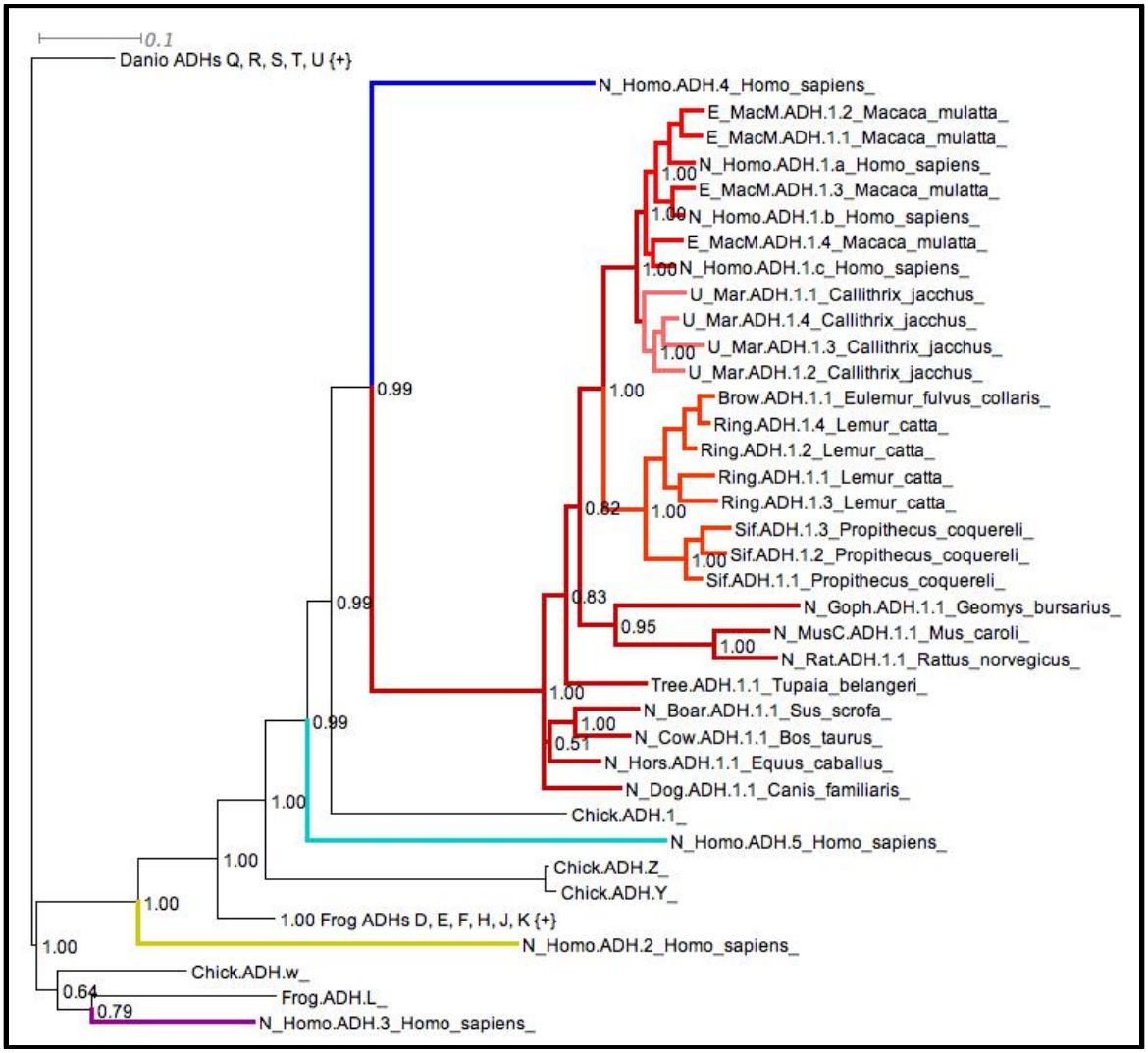

Figure 5. Phylogenetic relationship of *ADH1* paralogs as determined by Bayesian analysis of exonic sequence data using a codon model, including strepsirrhines (lemurs, orange); platyrrines (New World primates, pink), and catarrhines (Old World primates and hominoids, red). The human *ADH2*, *ADH3*, *ADH4* and *ADH5* genes were used as representatives for mammalian ADH Class I - V. Neither chicken (*Gallus gallus*) nor frog (*Xenopus tropicalis*) representatives of the mammalian ADH Class II proteins were found in the public nucleotide databases, suggesting that either (1) these genes have not yet been sequenced in both chicken and frog, (2) the ADH Class II homolog has been lost in both chicken and frog, or (3) the position of the human *ADH2* gene is incorrect in this tree (and should instead either be sister to human ADH3 or branch after the chicken ADH Z and ADH Y clade).

1. (Carrigan *et al.* 2012, unpublished)

Figure 6: Primate Evolutionary Divergence Timeline[1]

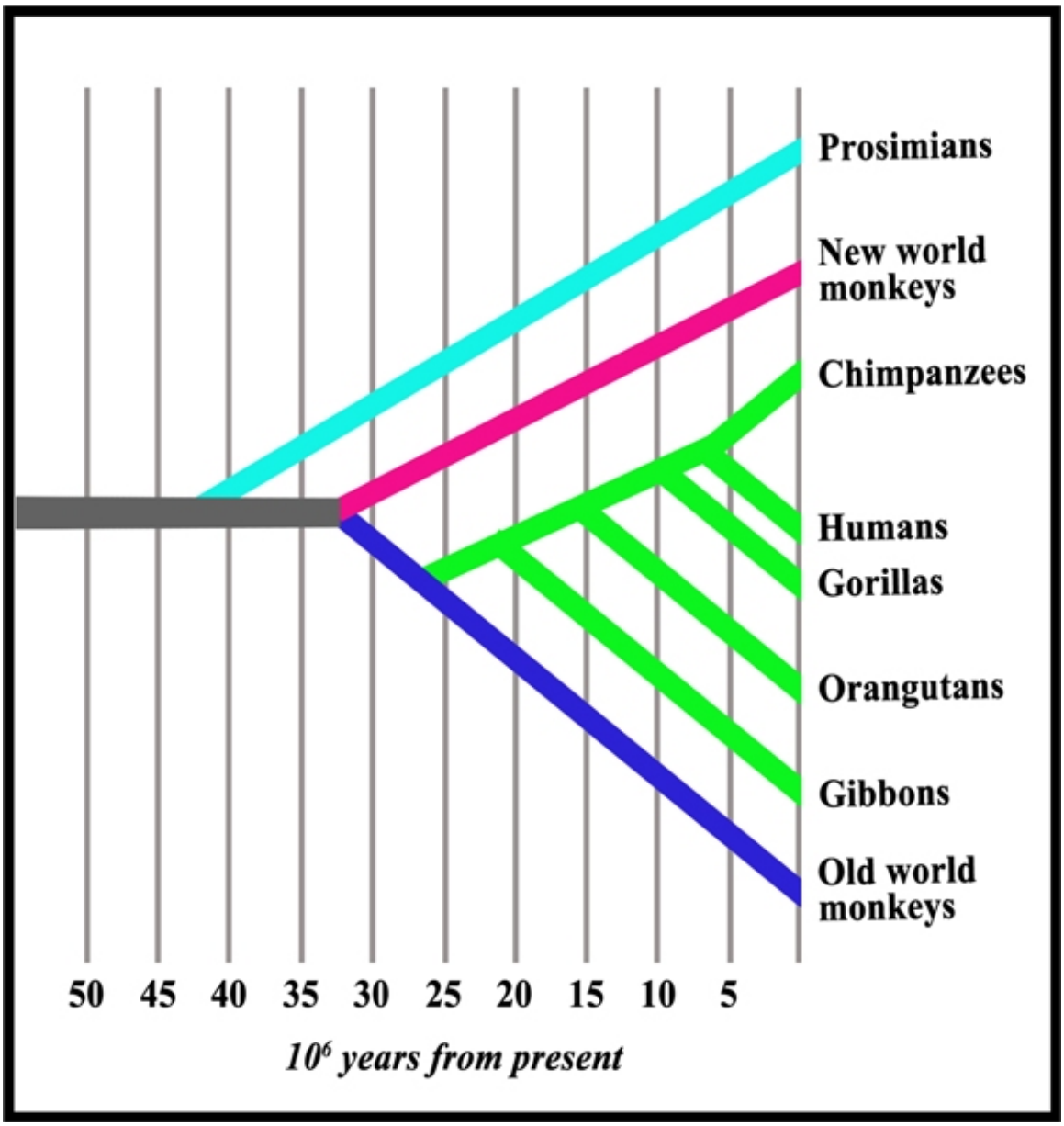

1. Figure derived from data in (Flotte *et al.* 2010).

Figure 7: Primate Cladogram displaying the Nodes from which Ancestral Class IV ADHs were resurrected

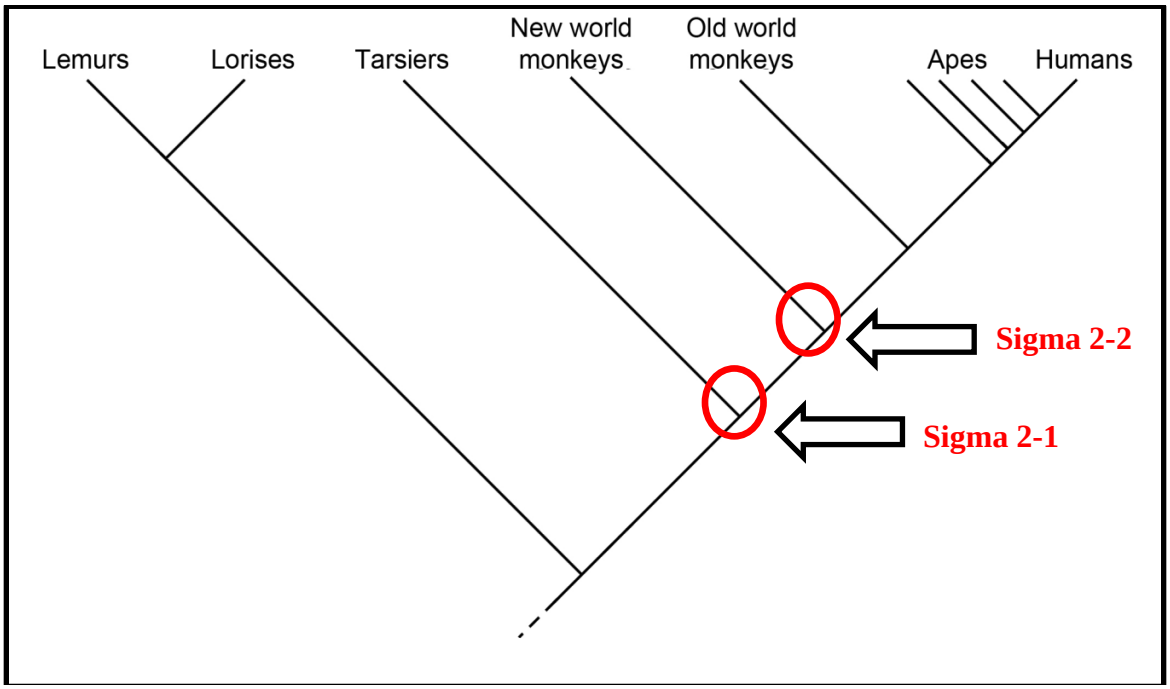

II. METHODS

1. Protein Purification

The Protein Expression Core Facility at IUPUI was responsible for preparing the vector designs and performing protein purification protocols for all enzymes used in experiments. ADH enzymes 4B, 22B, Sigma 2-1, and Sigma 2-2 were all expressed and purified following the same protocol—described below. The vector, pET41a-his, was used to express recombinant 4B, Sigma 2-1, and Sigma 2-2; while pET28a-his was used to express recombinant 22B.

Cultures of *E. coli* transformed with the appropriate expression vector were grown overnight at 37ºC in 20 ml of LB media (containing 50 µg/ml of Kanamycin). 20 ml of the overnight culture was then added to 1,000 ml of LB media (containing 50 µg/ml of Kanamycin), and allowed to grow at 37ºC to an OD_{600} of 0.5. Expression of the protein was induced by the addition of both IPTG (isopropyl-β-D-thiogalactopyranoside, 0.1 mM final concentration), and $ZnSO_4$ (to a final concentration of 10 µM); which was incubated at 16ºC for an additional 16 hours. The cells were then harvested by centrifugation, and the resulting pellet was stored at -80ºC.

In order to lyse the cells for protein purification, the cell pellet was thawed on ice, and cells were resuspended in 25 ml of lysis buffer (50 mM Tris, 0.3 M NaCl, 10 mM Imidazole, 2 mM Benzamidine [pH 8.0]). The resuspended cells were lysed by passage through a French Pressure cell operated at 13,000 psi; followed by centrifugation to clarify the lysate. The clarified lysate present in the supernatant was saved and transferred to a new tube for protein purification.

For protein purification, 2 ml of Ni-NTA-Superflow resin, equilibrated in lysis buffer, was added to the lysate supernatants and mixed gently by rotation at 4ºC for 2 hours. The resin was then centrifuged, the supernatant saved and then the resin was washed with three volumes of lysis buffer,and centrifuged again. Next, 40 ml of buffer A (50 mM Tris, 0.3 M NaCl, 20 mM Imidazole, 1 mM Benzamidine [pH 8.0]) was added to resuspend the Ni-NTA resin. This Ni-NTA mixture was then poured into a column, and washed with 50 ml of buffer A, and then with 100 ml of buffer B (50 mM Tris, 0.3 M NaCl, 30 mM Imidazole, 1 mM Benzamidine [pH 8.0]) to remove non-specifically bound proteins.. Finally, the ADH proteins were eluted with addition of four, 0.5-ml aliquots of Elution buffer (50 mM Tris, 0.3 M NaCl, 200 mM Imidazole, 1 mM Benzamidine [pH 8.0]).

The activities of the fractions were measured via spectrophotometer using standard ADH assays, and analyzed by SDS-PAGE. Fractions were then concentrated and buffer-exchanged with 10 mM Tris (pH 8.0), and 1 mM DTT—using a Micron 30 concentrator (Amicon, Beverly, MA). Protein was then either aliquotted and flash-freezed in liquid nitrogen (and stored at -80ºC), or aliquotted and stored at -20ºC in a 50% (v/v) glycerol solution. If stored in a glycerol solution, a gel-filtration column was used to remove glycerol before kinetic analysis.

2. Activity Assay and Enzyme Kinetics

A Beckman DU-640 spectrophotometer was used to monitor alcohol dehydrogenase activity for the enzymes. The spectrophotometer utilized an extinction coefficient of 6.22 $mM^{-1}cm^{-1}$ at 25ºC, for production of NADH at 340 nm.

The assay used for each experiment measured duplicate enzyme cuvettes, which contained final concentrations of the following reagents: 100 mM sodium phosphate (pH 7.5), 2.5mM NAD^+, alcohol substrate (0.015 mM-450.0 mM), and enzyme (16.8 µM-1030 µM). The blank cuvette, which was used for each measurement, contained all reagents in the reaction mixture *except* for the substrate. Reaction buffer (100 mM sodium phosphate [pH 7.5]) was prepared as-needed (typically every 3-4 weeks); and 75 mM NAD^+ was prepared daily with reaction buffer and added to the reaction cuvettes to yield final concentrations of 2.5 mM. Alcohol stock solutions were initially prepared with MilliPore grade H_2O. These stock solutions lasted throughout the duration of all experiments. Dilutions were made with reaction buffer from these stock solutions as needed—in order to obtain the desired final substrate concentrations. Stock solutions were made by diluting pure alcohols to yield final volumes of 100 ml each. Ethanol (58.69 ml/mol), which was purchased from AAPER Alcohol & Chemical Co. (Shelbyville, KY), was diluted to yield a final stock concentration of 1 M. Propanol (75.14 ml/mol) was diluted to yield a stock of 1 M; butanol (91.97 ml/mol) to 0.25 M; pentanol (108.63 ml/mol) to 0.05 M; hexanol (125.23 ml/mol) to 0.025 M; cyclohexanol (104.01 ml/mol) to 0.05 M, and *trans*-2-hexen-1-ol (129.8 ml/mol) to 0.025 M.

Reaction buffer, NAD^+, and the desired alcohol substrates were each added to cuvettes, respectively. The reaction was then initiated upon addition of enzyme. This addition allowed for the spectrophotometer to measure the rate of NADH production; determined by calculating the initial velocity during the first 60 seconds of the reaction.

The K_m and V_{max} values for each enzyme and substrate were calculated using the results from triplicate experiments. The calculated average V_{max} values were then

divided by the initial protein concentration added, and multiplied by mg/μmole of enzyme; thus resulting in units of μmoles of NADH produced per minute, per μmole of enzyme active sites. The data obtained from the spectrophotometer was in Units (U) per milliliter. The final V_{max} values were obtained with use of the following equations:

$$1 \text{ Unit (U)enzyme} = \frac{1 \text{ μmole NADH}}{\text{min}}$$

&

$$\frac{\frac{\text{U}}{\text{ml}}}{\frac{\text{mg}}{\text{ml}}} = \frac{\text{U}}{\text{mg}} = \frac{\text{μmoles/min}}{\text{mg}} \times \frac{40 \text{ mg (enzyme)}}{\text{μmole}}$$

A. 4B Assays

Substrates used in 4B experiments included the primary alcohols ethanol, propanol, butanol, pentanol, hexanol, and *trans*-2-hexen-1-ol, as well as the secondary alcohol cyclohexanol. Experiments for all substrates contained final protein concentrations of 0.75 μM, except for *trans*-2-hexen-1-ol—containing a final protein concentration of 0.25 μM. An ethanol stock solution of 1 M was used to create a 20 mM ethanol solution, which was then used to create ethanol experiments at concentrations of 0.15 mM, 0.25 mM, 0.50 mM, 1.0 mM, and 2.0 mM. A 20 mM propanol solution was used to create experiments at concentrations of 0.075 mM, 0.30 mM, 0.75 mM, 1.0 mM, and 2.5 mM. A 20 mM butanol solution was used to create experiments at concentrations of 0.10 mM, 0.40 mM, 1.0 mM, 2.0 mM, and 5.0 mM. A 20 mM pentanol solution was used to create experiments at concentrations of 0.10 mM, 0.40 mM, 1.0 mM, 2.0 mM, 5.0 mM, and 10.0 mM. A 20 mM hexanol solution was used to create experiments at concentrations of 0.10 mM, 0.40 mM, 1.0 mM, 2.0 mM, and 5.0 mM. A 50 mM

cyclohexanol solution was used to create experiments at concentrations of 5.0 mM, 7.5 mM, 10.0 mM, 20.0 mM, and 40.0 mM. A 2 mM *trans*-2-hexen-1-ol solution was used to create experiments at concentrations of 0.025 mM, 0.50 mM, 0.075 mM, 0.10 mM, 0.20 mM, 0.40 mM, and 1.0 mM.

B. 22B Assays

Substrates used in 22B experiments included the primary alcohols ethanol, propanol, butanol, pentanol, hexanol, and *trans*-2-hexen-1-ol, as well as the secondary alcohol cyclohexanol. All substrates utilized final 22B enzyme concentrations of 0.9 µM. A 20 mM ethanol solution was used to create ethanol experiments at concentrations of 3.0 mM, 5.0 mM, 7.5 mM, and 15.0 mM; while 1 M of ethanol stock solution was used to create ethanol experiments at concentrations of 20.0 mM and 40.0 mM. A 10 mM propanol solution was used to create propanol experiments at concentrations of 0.25 mM, 0.50 mM, 0.75 mM, and 1.5 mM; while 20 mM of propanol solution was used to create experiments at concentrations of 3.0 mM and 8.0 mM. A 10 mM butanol solution was used to create butanol experiments at concentrations of 0.20 mM, 0.30 mM, 0.60 mM, 1.0 mM, 1.25 mM, and 2.0 mM. A 10 mM pentanol solution was used to create pentanol experiments at concentrations of 0.25 mM, and 0.35 mM; while 50 mM pentanol stock solution was used to create pentanol experiments at concentrations of 0.60 mM, 1.25 mM, and 2.0 mM. A 20 mM hexanol solution was used to create hexanol experiments at concentrations of 0.10 mM, 0.20 mM, 0.30 mM, 0.60 mM, 1.0 mM, and 2.0 mM. A 25 mM cyclohexanol solution was used to create cyclohexanol experiments at concentrations of 0.50 mM, 1.5 mM, 3.0 mM, 5.0 mM, and 5.5 mM. A 2 mM *trans*-2-hexen-1-ol solution was used to create *trans*-2-hexen-1-ol experiments at concentrations

of 0.015 mM, 0.02 mM, 0.025 mM, and 0.04 mM; while a 10 mM *trans*-2-hexen-1-ol solution was used to create *trans*-2-hexen-1-ol experiments at concentrations of 0.05 mM, and 0.10 mM.

C. Sigma 2-1 Assays

Substrates used in Sigma 2-1 experiments included only the primary alcohols ethanol, propanol, butanol, pentanol, hexanol, and *trans*-2-hexen-1-ol. Ethanol, propanol, and butanol experiments used final protein concentrations of 0.41 µM; pentanol and hexanol experiments used final protein concentrations of 1.03 µM; and *trans*-2-hexen-1-ol experiments used final protein concentrations of 0.02 µM. A 1 M ethanol stock solution was used to create ethanol experiments at concentrations of 25.0 mM, 80.0 mM, 175.0 mM, 275.0 mM, and 350.0 mM. A 1 M propanol stock solution was used to create propanol experiments at concentrations of 80.0 mM, 175.0 mM, 275.0 mM, 350.0 mM, and 450.0 mM. A 250 mM butanol stock solution was used to create butanol experiments at concentrations of 50.0 mM, 100.0 mM, 150.0 mM, 200.0 mM, and 225.0. A 50 mM pentanol stock solution was used to create pentanol experiments at concentrations of 2.5 mM, 10.0 mM, 25.0 mM, 35.0 mM, and 45.0 mM. 25 mM of hexanol stock solution was used to create hexanol experiments at concentrations of 1.0 mM, 2.5 mM, 5.0 mM, 15.0 mM, and 23.0 mM. A 25 mM *trans*-2-hexen-1-ol stock solution was used to create *trans*-2-hexen-1-ol experiments at concentrations of 0.10 mM, 0.50 mM, 2.0 mM, 5.0 mM, and 10.0 mM.

D. Sigma 2-2 Assays

Substrates used in Sigma 2-2 experiments included only the primary alcohols ethanol, propanol, butanol, pentanol, hexanol, and *trans*-2-hexen-1-ol. Ethanol,

propanol, and butanol experiments had final protein concentrations of 0.20 µM; pentanol experiments had final protein concentrations of 0.10 µM; hexanol and *trans*-2-hexen-1-ol experiments had final protein concentrations of 0.017 µM. A 500 mM ethanol solution was used to create ethanol experiments at concentrations of 15.0 mM, 35.0 mM, 55.0 mM, 75.0 mM, 100.0 mM and 140.0 mM. A 500 mM propanol solution was used to create propanol experiments at concentrations of 15.0 mM, 35.0 mM, 55.0 mM, 75.0 mM, 100.0 mM and 140.0 mM. A 250 mM butanol stock solution was used to create butanol experiments at concentrations of 15.0 mM, 20.0 mM, 30.0 mM, 60.0 mM, 90.0 mM, and 140.0 mM. A 50 mM pentanol stock solution was used to create pentanol experiments at concentrations of 1.0 mM, 2.5 mM, 10.0 mM, 15.0 mM, 20.0 mM and 35.0 mM. A 25 mM hexanol stock solution was used to create hexanol experiments at concentrations of 1.0 mM, 2.5 mM, 5.0 mM, 10.0 mM, 15.0 mM and 23.0 mM. A 2 mM *trans*-2-hexen-1-ol solution was used to create *trans*-2-hexen-1-ol experiments at concentrations of 0.10 mM, 0.30 mM, 0.50 mM, 1.0 mM, 3.0 mM, and 5.0 mM.

3. Analysis of Steady-State Kinetic Parameters

Data obtained from the kinetic experiments was fit to the Michaelis-Menton equation displayed below, using the software package Sigma Plot Enzyme Kinetics Package (Version 10.0):

$$v = \frac{V_{max} \times [S]}{K_m + [S]}$$

4. Reagents

All reagents used were purchased from Sigma-Aldrich (St. Louis, MO); unless otherwise noted.

5. Modeling

Modeling of the ADH isoenzymes was performed using Swiss-PdbViewer (Version 4.0.4) and PyMOL (Version 1.4.1) and either the coordinates of human $\beta_1\beta_1$ alcohol dehydrogenase complexed with coenzyme and heptylformamide (RCSB code 1U3V), human $\gamma_2\gamma_2$ alcohol dehydrogenase complexed with coenzyme and methylheptylformamide (RCSB code 1U3W) or human $\sigma\sigma$ alcohol dehydrogenase (RCSB code 1D1S). Human ADH amino acid sequences were manipulated by substituting amino acids at positions in the substrate binding site in order to correspond to sequences from brown lemur, marmoset, and human ancestral isoenzymes. Next, respective sequences were generated in Swiss-PdbViewer using the *mutate* function and utilizing the *rotamer* selection to minimize contacts with surrounding residues. The final models/figures were generated using PyMOL and used to demonstrate structural similarities and differences between select isoenzymes.

6. Determining Class I ADH Genes among Primates

The NCBI website was used to determine the number and type of Class I ADH genes present among various existing primates by first performing a protein search for human (*ADH1A*, *ADH1B*, or *ADH1C*), and then performing sequence match searches for respective isoenzymes via BLAST. Results demonstrating at least 85% sequence identity between species were considered to be matches (homologous).

III. RESULTS

1. Enzymes: 2M, 10M, 4B, and 22B

A. Ethanol, Propanol, Butanol, Pentanol, and Hexanol as Substrates

For the 2M isoenzyme from Marmoset, the values for K_m, V_{max}, and V_{max}/K_m (catalytic efficiency) amongst the primary aliphatic alcohols (ethanol, propanol, butanol, pentanol, and hexanol) were relatively constant, varying by a maximum of 2-fold within each group of kinetic constant [Tables 7-9]. The K_m values from ethanol to hexanol remained almost constant at 0.79 and 0.81 mM for ethanol and hexanol, respectively [Table 7]. Similarly, the V_{max} values for ethanol, propanol, and butanol remained constant, but the V_{max} for pentanol and hexanol decreased by approximately 25% [Table 8]. Not surprisingly, given the constancy of the individual values, the catalytic efficiencies for these substrates varied merely 1.4-fold [Table 9].

In contrast to the 2M ADH isoform, the 10M isoenzyme from marmoset exhibited K_m values that varied in a chain-length dependent manner with a K_m for ethanol that was 12-fold higher than that for hexanol [Table 7]. Similarly, the V_{max} also decreased with increasing chain length—with the V_{max} for ethanol oxidation exceeding that of hexanol oxidation by nearly 4-fold [Table 8]. The trend in V_{max}/K_m for these primary alcohols increased as substrate chain-length increased—yielding 3.8-fold higher values for pentanol and hexanol compared to that for ethanol [Table 9].

A similar trend was observed with the two ADH isoforms from brown lemur (4B and 22B); where one isoenzyme exhibited no large changes in the kinetic constants for the aliphatic alcohols, and one enzyme which demonstrated chain-length dependence for these kinetic constants [Tables 7-9]. The K_m, V_{max}, and V_{max}/K_m values for the 4B

isoenzyme for these primary alcohols were relatively constant—varying by a maximum of only 2-fold per category. K_m values increased from ethanol to butanol by about 2-fold, but then decreased again from butanol to hexanol; such that ethanol and hexanol possessed similar K_m values [Table 7]. The V_{max} for ethanol and propanol were similar, while the V_{max} decreased with increasing chain length after propanol. There was about a 2-fold decrease in the V_{max} for hexanol oxidation compared to that for ethanol/propanol [Table 8; Figure 8]. The catalytic efficiencies varied by a maximum of 2-fold; ethanol and propanol were similar, while butanol was decreased 2-fold relative to propanol. Both pentanol and hexanol had higher catalytic efficiencies than butanol, but lower efficiencies than ethanol and propanol [Table 9].

Like the 10M isoenzyme, the 22B isoenzyme exhibited K_m values that ranged by 30-fold; with values decreasing with increasing substrate chain length [Table 7]. The K_m value for propanol dropped 8-fold relative to ethanol; while the K_m values for both butanol and pentanol decreased by about 11-fold relative to ethanol. The K_m value for hexanol as a substrate was the lowest; decreasing 30-fold relative to that of ethanol. Unlike the 10M isoenzyme, the V_{max} values for 22B remained relatively constant, varying only 1.2-fold [Table 8; Figure 9]. Given the consistency of the V_{max} values, the changes in the catalytic efficiencies for the 22B isoenzyme were driven by the differences in K_m for the substrate, and were 26-fold higher for hexanol than for ethanol [Table 9]. The catalytic efficiencies increased about 8-fold from ethanol to propanol; then increased about 1.5-fold from propanol to butanol/pentanol, and increased again by about 2-fold from butanol/pentanol to hexanol.

B. Cyclohexanol as a Substrate

Cyclohexanol was a highly variable substrate for these isoenzymes; with some almost preferring this secondary alcohol (10M) and others barely oxidizing it (4B). The 2M isoenzyme was the second best toward cyclohexanol oxidation, but it was the poorest substrate tested with this isoenzyme. The 2M isoenzyme exhibited a K_m value that was 2-fold higher, compared to that of primary alcohol substrates, a decreased V_{max} (about 2-fold lower than ethanol, propanol, and butanol; but only 25% lower than for pentanol/hexanol); and a 4- to 5-fold decrease in V_{max}/K_m compared to those of primary alcohols [Tables 7-9].

The 10M isoenzyme was the best enzyme for oxidation of cyclohexanol; where the K_m value for cyclohexanol was comparable to that of hexanol and pentanol, and about 12-fold lower than for that of ethanol [Table 7]. The V_{max} for cyclohexanol oxidation was slightly lower than for ethanol oxidation, and about 3-fold higher than for hexanol [Table 8]. The catalytic efficiency increased significantly with cyclohexanol, and was 3-fold higher than for the oxidation of pentanol or hexanol; and 11-fold higher than for ethanol [Table 9].

The 4B isoenzyme was the poorest enzyme for cyclohexanol oxidation. The K_m value for cyclohexanol was increased approximately 40-fold compared to the K_m values for the primary alcohols [Table 7]. The V_{max} for cyclohexanol oxidation was not as adversely affect and was comparable to that of hexanol: approximately 2-fold lower than that of ethanol or propanol [Table 8; Figure 10-A]. The V_{max}/K_m for cyclohexanol decreased substantially compared to the V_{max}/K_m for primary alcohols ranging from 58-fold lower than butanol, to 125-fold lower than ethanol [Table 9].

The 22B and 2M ADH isoenzymes had similar catalytic efficiencies for cyclohexanol; but unlike the 2M isoenzyme, cyclohexanol was not the worst substrate tested for the 22B isoenzyme. The 22B isoenzyme exhibited a K_m value that was increased about 4-fold lower than ethanol, but about 2-fold higher than propanol [Table 7]. The V_{max} for cyclohexanol oxidation was slightly lower than all primary alcohols, but within statistical error of most of the primary alcohol oxidation rates [Table 8; Figure 10-B]. The catalytic efficiency for cyclohexanol oxidation was about 4-fold higher than that of ethanol, but decreased between 2- and 7-fold relative to the aliphatic primary alcohols [Table 9].

C. Trans-2-hexen-1-ol as a Substrate

The unsaturated primary alcohol, *trans*-2-hexen-1-ol, was the best substrate for all primate Class I isoenzymes tested. When used as a substrate for the 2M isoenzyme, the K_m for this substrate was approximately 6- to 10-fold lower than that of the primary alcohols, including hexanol, its closest structural analog, and was about 20-fold lower than for cyclohexanol [Table 7]. The V_{max} measured with *trans*-2-hexen-1-ol as a substrate was higher than that of all primary alcohols—increasing by a maximum of about 2-fold (relative to pentanol/hexanol) [Table 8]. The V_{max}/K_m for *trans*-2-hexen-1-ol increased significantly compared to the catalytic efficiencies for the primary alcohols (12-17 fold increases), and about 58-fold higher than that of cyclohexanol as a substrate [Table 9].

For the 10M isoenzyme, the K_m value for *trans*-2-hexen-1-ol was equal to the values for both hexanol and cyclohexanol; while the K_m was decreased approximately 12-fold relative to ethanol [Table 7]. The V_{max} measured for *trans*-2-hexen-1-ol as a

substrate was higher than those of all of the primary alcohols (up to 5-fold higher than for hexanol oxidation, but only 1.4-fold higher than for cyclohexanol oxidation [Table 8]. The V_{max}/K_m for *trans*-2-hexen-1-ol as a substrate was higher than the catalytic efficiencies for all primary alcohols, as well as for cyclohexanol—ranging from a 4- to a 15-fold increase [Table 9]. The catalytic efficiency for *trans*-2-hexen-1-ol also increased about 1.5-fold compared to that of cyclohexanol.

When *trans*-2-hexen-1-ol was used as a substrate for the 4B isoenzyme, the K_m value was approximately 18-fold lower than K_m values for the other primary alcohols, and 1000-fold lower than for cyclohexanol [Table 7]. In contrast, the V_{max} value was similar to that of ethanol and propanol oxidation and approximately 2-fold higher than for that of hexanol and cyclohexanol oxidation [Table 8; Figure 11-A]. The V_{max}/K_m value for *trans*-2-hexen-1-ol oxidation was 15 to 33-fold higher than the catalytic efficiencies for primary alcohols and over 1900-fold higher than the catalytic efficiencies for cyclohexanol oxidation [Table 9].

When *trans*-2-hexen-1-ol was used as a substrate for the 22B isoenzyme, the K_m value was lower compared to all primary alcohols (between 9-fold and 260-fold lower) and 60-fold lower than the K_m for cyclohexanol [Table 7]. Similar to the behavior of the other primate isoenzymes, the V_{max} for *trans*-2-hexen-1-ol oxidation was higher than for any other substrate tested with increases 1.5-fold compared to all primary alcohols and about 1.8-fold compared to cyclohexanol [Table 8; Figure 11-B]. The V_{max}/K_m value for *trans*-2-hexen-1-ol was higher than the catalytic efficiencies for all other primary alcohols (between 15- and 400-fold higher) and about 100-fold higher than for cyclohexanol [Table 9].

2. Enzymes: Sigma 2-1 and Sigma 2-2

A. Ethanol, Propanol, Butanol, Pentanol, and Hexanol as Substrates

Kinetic constants for both of the resurrected primate ADH isoforms, Sigma 2-1 and Sigma 2-2, demonstrated similar trends in values for K_m, V_{max}, and V_{max}/K_m (catalytic efficiency) amongst primary aliphatic alcohols. The Sigma 2-1 isoenzyme exhibited K_m values that varied in a chain-length dependent manner—increasing 1.3-fold from ethanol to propanol, then decreasing 92-fold from propanol to hexanol [Table 10]. In contrast, V_{max} values increased as chain-length increased; demonstrating a 3.1-fold increase from ethanol to pentanol, and a 1.4-fold decrease from pentanol to hexanol [Table 11; Figure 12]. Catalytic efficiencies amongst primary aliphatic alcohols increased with increasing chain-length as well; where the V_{max}/K_m for ethanol and propanol were relatively constant, differing by a mere 1.3-fold, followed by a 130-fold increase from propanol to hexanol [Table 12].

Similar to Sigma 2-1, the Sigma 2-2 isoenzyme displayed K_m, V_{max}, and V_{max}/K_m values (catalytic efficiencies) that varied in a chain-length dependent manner. Sigma 2-2 also exhibited K_m values which increased slightly from ethanol to propanol (1.2-fold), then decreased with increasing chain length from propanol to hexanol (170-fold) [Table 10]. Contrary to Sigma 2-1, Sigma 2-2 exhibited V_{max} values which continuously increased from ethanol to hexanol, displaying a 4-fold increase from ethanol to hexanol [Table 11; Figure 13]. Much like Sigma 2-1, catalytic efficiencies for isoenzyme Sigma 2-2 remained constant from ethanol and propanol then increased with increasing chain length from propanol to hexanol (590-fold increase) [Table 12].

B. Trans-2-hexen-1-ol as a Substrate

For both resurrected primate isoenzymes (Sigma 2-1 and Sigma 2-2) the unsaturated primary alcohol, *trans*-2-hexen-1-ol, was the best substrate. For Sigma 2-1, the K_m was lowest for *trans*-2-hexen-1-ol—demonstrating a 710-fold decrease compared to that for propanol, and a 7.7-fold decrease compared to that for hexanol [Table 10]. The V_{max} for *trans*-2-hexen-1-ol was also higher than all primary aliphatic alcohols tested; exhibiting a 7-fold increase compared to that for pentanol, and a 22-fold increase compared to that for ethanol [Table 11; Figure 11-C]. As expected, given the low K_m and high V_{max} values obtained, the catalytic efficiency for *trans*-2-hexen-1-ol increased 77-fold compared to that for hexanol, and increased 12,000-fold compared to that for ethanol [Table 12].

For Sigma 2-2, K_m values were lowest for *trans*-2-hexen-1-ol—demonstrating a 1100-fold decrease compared to that for propanol, and a 6.5-fold decrease compared to that for hexanol [Table 10]. Likewise, the V_{max} for trans-2-hexen-1-ol was higher than all primary aliphatic alcohols tested; exhibiting a 5.4-fold increase compared to that for pentanol, and a 22-fold increase compared to that for ethanol [Table 11; Figure 11-D]. The catalytic efficiency for *trans*-2-hexen-1-ol exhibited a 33-fold increase compared to that for hexanol, and a 20,000-fold increase compared to that for ethanol [Table 12].

Table 7: K_m Constants (mM) of ADH Isoenzymes from Brown Lemur[1] and Marmoset[2] at pH 7.5

	Primate ADH isoenzymes →	4B[1]	22B[1]	2M[2]	10M[2]
SUBSTRATES	Ethanol	0.55 +/- 0.08	9.5 +/- 1.0	0.79 +/- 0.10	0.73 +/- 0.05
	Propanol	0.64 +/- 0.09	1.1 +/- 0.1	0.95 +/- 0.12	0.39 +/- 0.05
	Butanol	1.1 +/- 0.1	0.84 +/- 0.14	1.2 +/- 0.4	0.10 +/- 0.02
	Pentanol	0.74 +/- 0.03	0.82 +/-0.14	0.61 +/- 0.09	0.07 +/- 0.01
	Hexanol	0.47 +/- 0.03	0.32 +/- 0.07	0.81 +/- 0.21	0.06 +/- 0.01
	Trans-2-hexen-1-ol	0.038 +/- 0.003	0.037 +/- 0.003	0.10 +/- 0.04	0.06 +/- 0.02
	Cyclohexanol	40 +/- 14	2.2 +/- 0.6	2.1 +/- 0.13	0.06 +/- 0.00

Table 8: V_{max} Constants (min^{-1}) of ADH Isoenzymes from Brown Lemur[1] and Marmoset[2] at pH 7.5

	Primate ADH isoenzymes →	4B[1]	22B[1]	2M[2]	10M[2]
SUBSTRATES	Ethanol	17 +/- 1	12 +/- 1	23 +/- 1	22 +/- 1
	Propanol	18 +/- 2	12 +/- 1	22 +/- 1	15 +/- 1
	Butanol	15 +/- 1	12 +/- 1	29 +/- 6	9 +/- 1
	Pentanol	12 +/- 1	12 +/- 1	16 +/- 1	8 +/- 1
	Hexanol	9.8 +/- 0.2	10 +/- 1	17 +/- 2	6 +/- 1
	Trans-2-hexen-1-ol	18 +/- 1	18 +/- 1	35 +/- 10	28 +/- 6
	Cyclohexanol	9.7 +/- 1.9	9.8 +/- 0.8	12 +/- 1	20 +/- 1

Table 9: V_{max}/K_m values ($min^{-1}mM^{-1}$) of ADH Isoenzymes from Brown Lemur[1] and Marmoset[2] at pH 7.5

	Primate ADH isoenzymes →	4B[1]	22B[1]	2M[2]	10M[2]
SUBSTRATES	Ethanol	30	1.2	29	30
	Propanol	29	10	23	38
	Butanol	14	15	24	90
	Pentanol	17	15	26	110
	Hexanol	21	32	21	100
	Trans-2-hexen-1-ol	460	480	350	470
	Cyclohexanol	0.24	4.5	6	330

(All data was rounded to 2 significant figures.)

2. 2M and 10M (unpublished) data was obtained from Hina Younus (previous graduate student)

Table 10: K_m Constants (mM) of Ancestral[1] and Human[2] ADH Isoenzymes at pH 7.5

	ADH isoenzymes →	Sigma 2-1[1]	Sigma 2-2[1]	σσ[2]
SUBSTRATES	Ethanol	360 +/- 71	310 +/- 73	28
	Propanol	470 +/- 200	370 +/- 13	1.4
	Butanol	86 +/- 7	31 +/- 9	0.79
	Pentanol	14 +/- 1	8.3 +/- 0.8	0.28
	Hexanol	5.1 +/- 1.7	2.2 +/- 0.6	0.13
	Trans -2-hexen-1-ol	0.66 +/- 0.04	0.34 +/- 0.02	0.019

Table 11: V_{max} Constants (min^{-1}) of Ancestral[1] and Human[2] ADH Isoenzymes at pH 7.5

	ADH isoenzymes →	Sigma 2-1[1]	Sigma 2-2[1]	σσ[2]
SUBSTRATES	Ethanol	180 +/- 32	250 +/- 37	1,800
	Propanol	300 +/- 54	310 +/- 13	1,000
	Butanol	360 +/- 10	420 +/- 38	2,100
	Pentanol	560 +/- 21	530 +/- 9	960
	Hexanol	390 +/- 48	1,000 +/- 64	1,200
	Trans -2-hexen-1-ol	3,900 +/- 64	5,400 +/- 64	2,200

Table 12: V_{max}/K_m Values ($min^{-1}mM^{-1}$) of Ancestral[1] and Human[2] ADH Isoenzymes at pH 7.5

	ADH isoenzymes →	Sigma 2-1[1]	Sigma 2-2[1]	σσ[2]
SUBSTRATES	Ethanol	0.49	0.82	65
	Propanol	0.64	0.82	570
	Butanol	4.2	13	2,600
	Pentanol	39	64	3,400
	Hexanol	78	480	9,000
	Trans -2-hexen-1-ol	6,000	16,000	120,000

(All data was rounded to 2 significant figures.)

2. Data from (Kedishvili *et al.* 1995)

Figure 8: Michaelis-Menten Representative Graphs of 4B-ADH from Brown Lemur with Various Aliphatic Alcohols[1]

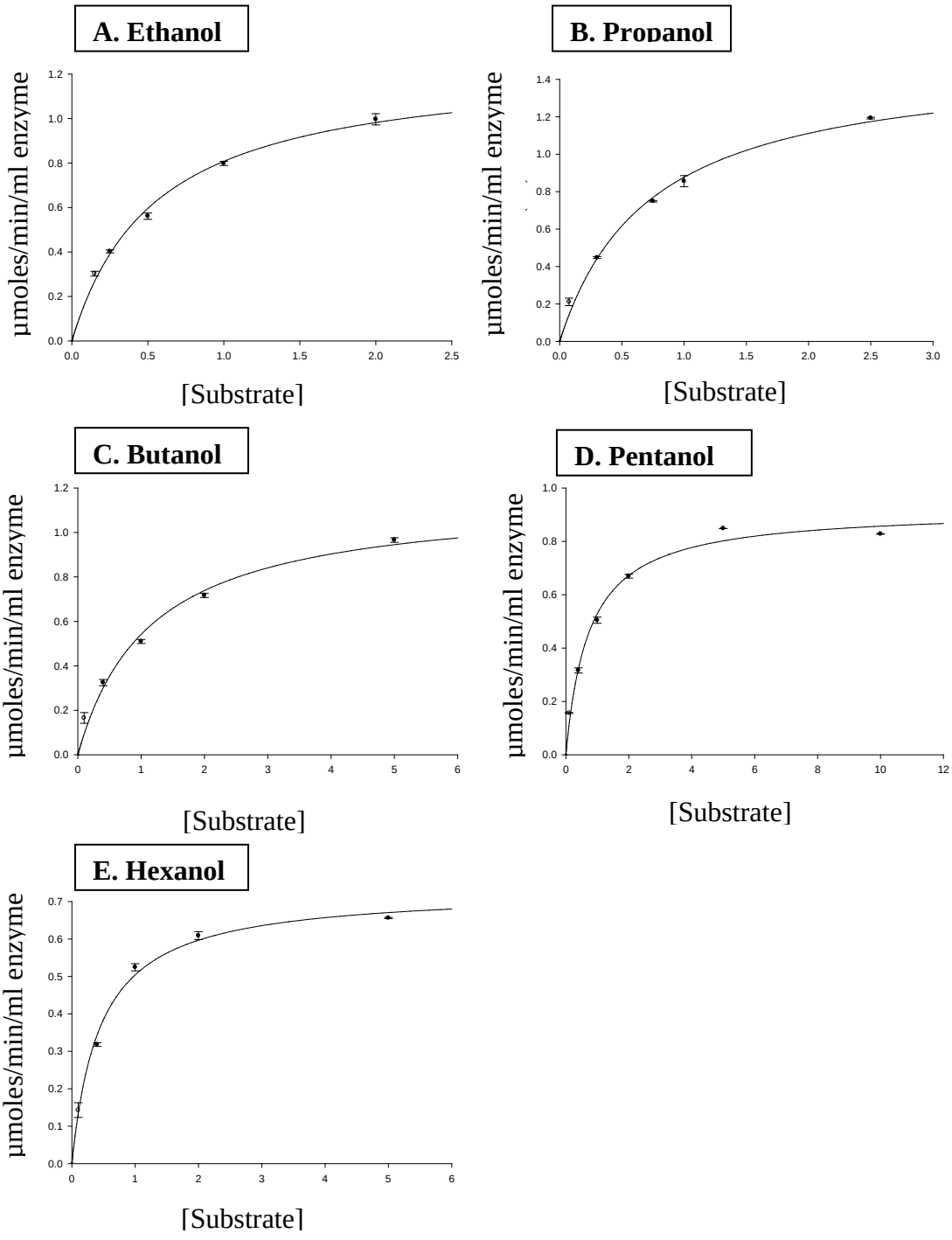

1. Data points represent the average of triplicate measurements recorded +/- standard error—which is represented by a vertical line through each data point.

Figure 9: Michaelis-Menten Representative Graphs of 22B-ADH from Brown Lemur with Various Aliphatic Alcohols[1]

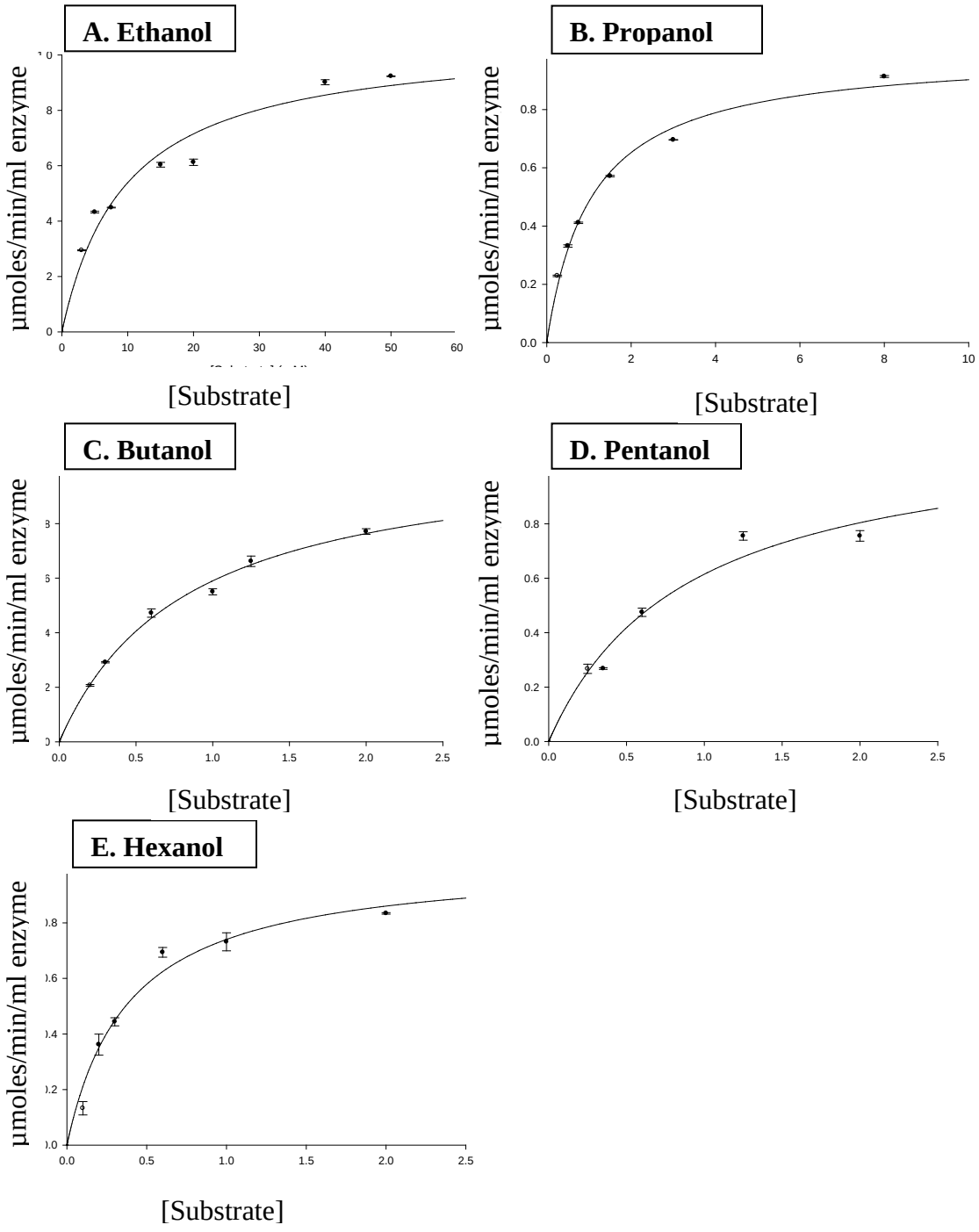

1. Data points represent the average of triplicate measurements recorded +/- standard error—which is represented by a vertical line through each data point.

Figure 10: Michaelis-Menten Representative Graphs of Brown Lemur ADHs with Cyclohexanol[1]

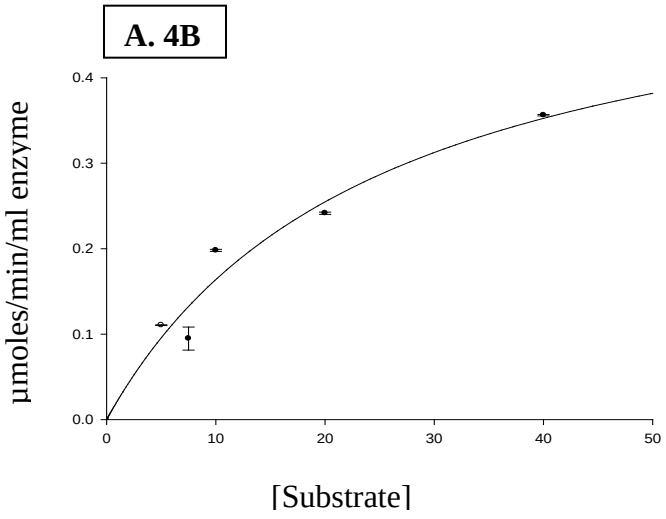

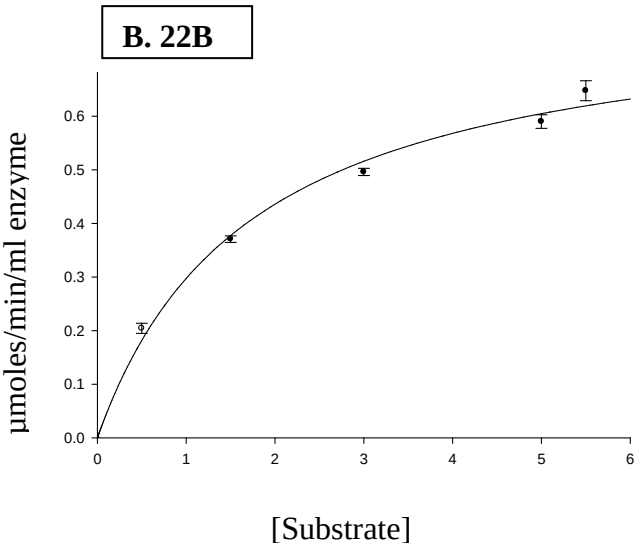

1. Data points represent the average of triplicate measurements recorded +/- standard error—which is represented by a vertical line through each data point.

Figure 11: Michaelis-Menten Representative Graphs of Primate and Ancestral ADHs with *Trans*-2-hexen-1-ol as a Substrate.[1]

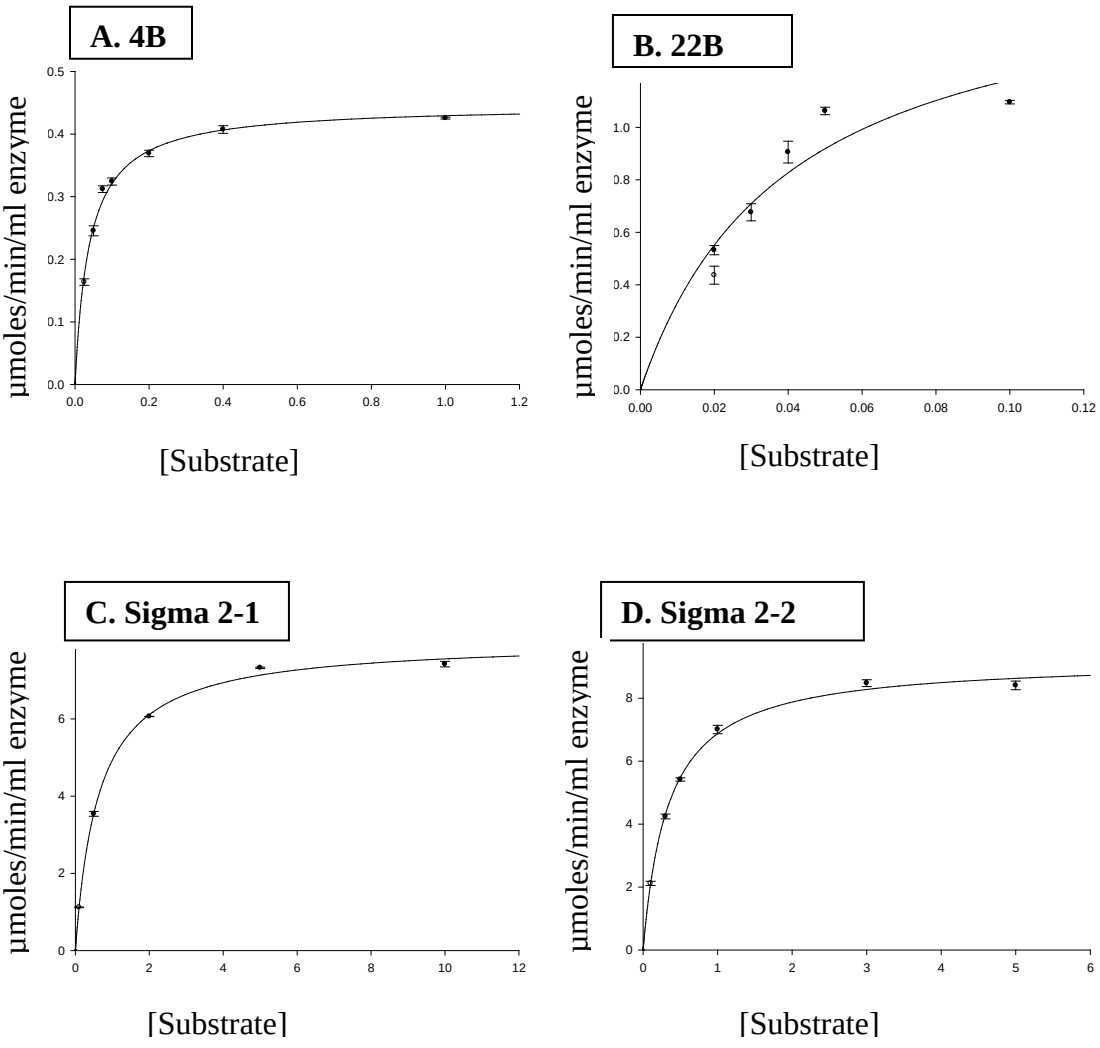

1. Data points represent the average of triplicate measurements recorded +/- standard error—which is represented by a vertical line through each data point.

Figure 12: Michaelis-Menten Representative Graphs of Ancestral, Sigma 2-1 ADH with Various Aliphatic Alcohols.[1]

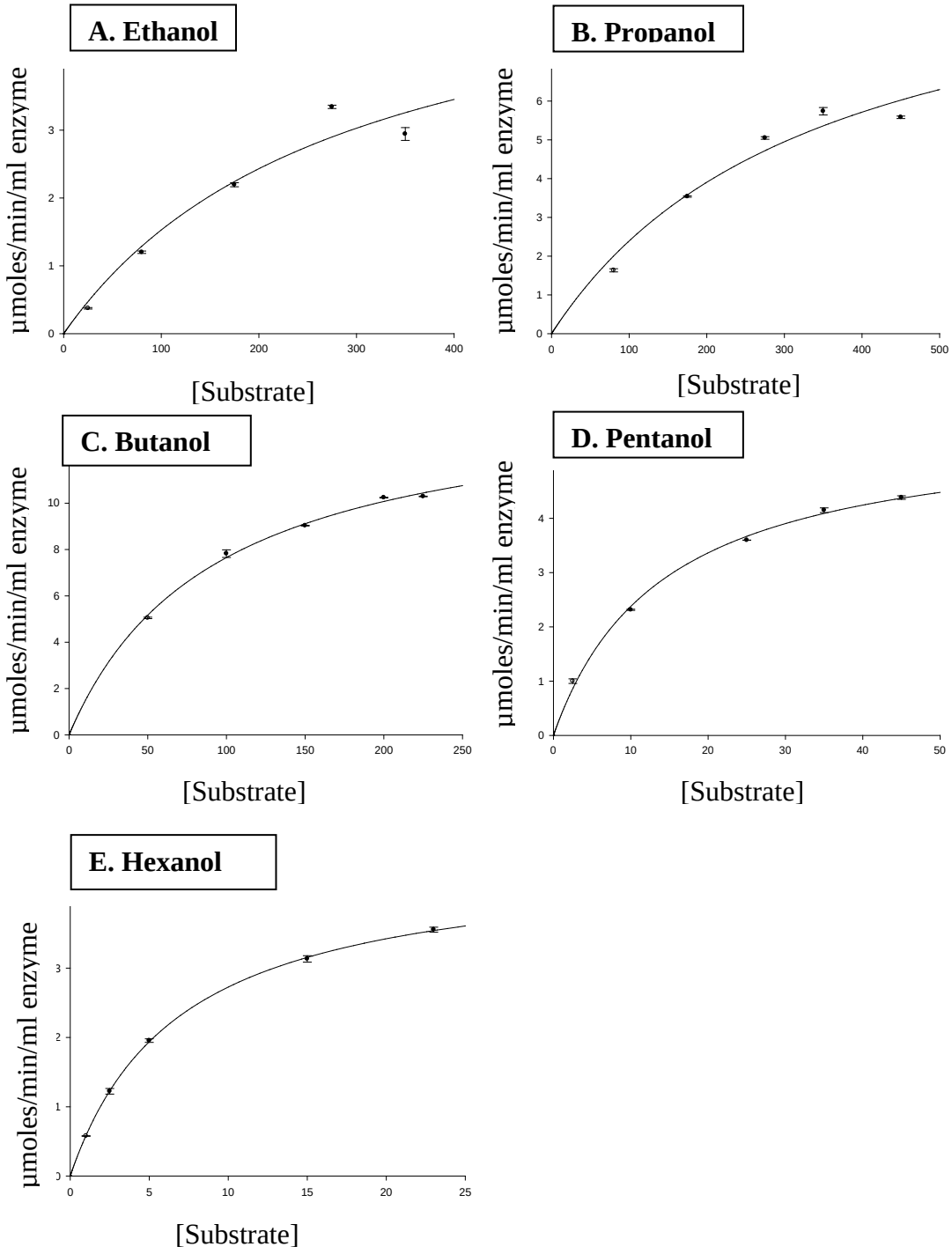

1. Data points represent the average of triplicate measurements recorded +/- standard error—which is represented by a vertical line through each data point.

Figure 13: Michaelis-Menten Representative Graphs of Ancestral, Sigma 2-2 ADH with Various Aliphatic Alcohols.[1]

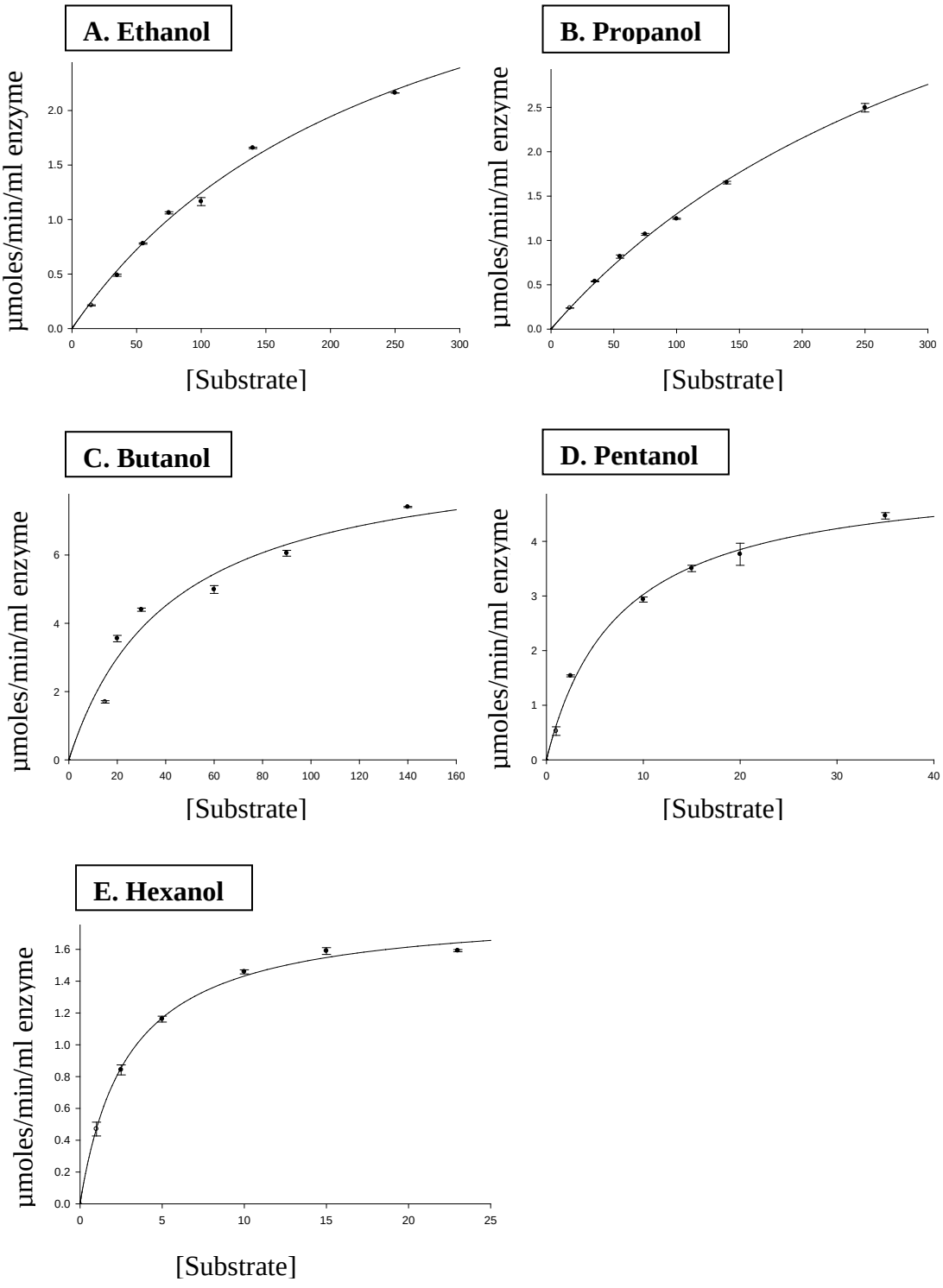

1. Data points represent the average of triplicate measurements recorded +/- standard error—which is represented by a vertical line through each data point.

IV. DISCUSSION

1. Background/ Review of ADH Genes and Isoenzymes

Alcohol dehydrogenase, encoded by the ADH gene family, is an enzyme that metabolizes various substrates: including ethanol, retinol, other aliphatic alcohols, hydroxysteroids, and lipid peroxidation products (Duester *et al.* 1999). ADH isoenzymes exist in four biological kingdoms: bacteria, yeast, plants, and animals (Branden *et al.* 1975). Human ADH isoenzymes are zinc-containing dimers consisting of two 40-kD subunits [Figure 1]. Each subunit, containing a structural zinc ion and a catalytic zinc ion, is folded into two domains: a coenzyme-binding domain and a catalytic domain. These domains are separated by a cleft containing a deep pocket—which accommodates the substrate and the nicotinamide moiety of the coenzyme. Homologous interactions within the coenzyme binding domains of each subunit link the dimers together (Eklund *et al.* 1976).

Seven alcohol dehydrogenase (ADH) genes have been identified in humans—*ADH1A*, *ADH1B*, *ADH1C*, *ADH4*, *ADH5*, *ADH7*, and *ADH6* (Hurley *et al.* 2002). This seven-gene cluster is found on chromosome four in humans (Edenberg 2000). ADH isoenzymes are classified into individual classes based on function and sequence identity (Duester 1999; Edenberg 2000). There is currently some disagreement amongst investigators and the Human Genome Organization (HUGO) concerning gene nomenclature assignments. This thesis will utilize the HUGO assignments. However the current literature can be confusing depending on which nomenclature is utilized (for review, see Duester 1999 and Hurley *et al.* 2002). In humans, the Class I isoenzymes are encoded by genes *ADH1A*, *ADH1B*, and *ADH1C*—which yield the protein products α, β,

an γγ, respectively. Polymorphisms occur at the *ADH1B* and *ADH1C* loci with different distributions amongst racial populations, giving rise to the *ADH1B*1*, *ADH1B*2*, and *ADH1B*3* alleles and the *ADH1C*1* and *ADH1C*2* alleles (Hurley *et al.* 2002). Class II, encoded by human *ADH4*, yields the protein product π; Class III, encoded by human *ADH5*, yields χ; and Class IV, encoded by human *ADH7* yields σ (Duester 1999). The Class V isoenzyme, human *ADH6* has only been identified at the gene and transcriptional level—and its function remains unknown (Hoog & Ostberg 2011).

On an evolutionary scale, human Class III and Class II ADHs probably diverged around 630 and 600 million years ago, respectively; while human Class IV appeared 520 million years ago—implying that these classes of enzymes may exist or have existed in all vertebrates. However, human Class I ADHs diverged 80 million years ago—before human, baboon, and monkey Class I ADHs—which is also when angiosperms first began to produce fleshy fruits whose sugars are fermented to ethanol by yeasts. This supports the proposal that duplications of the primate Class I gene could have predated primate radiation. Thus, human Class I ADH isoenzymes may exist or have existed in all primates (Sun & Plapp 1992).

It has been speculated that the highly conserved sequences on the three duplicated (Class I) ADH genes in primates have been achieved essentially by maintaining stability of the hetero-dimer formation that might have been related to dietary adaptation in primate evolution. Or in other words, this implies that the evolution of Class I ADH genes is associated with dietary adaptations in the primate lineage (Oota *et al.* 2007). Tables 1, 2 and 3 can be analyzed to demonstrate that the duplication of Class I ADH to

yield three two or three unique isoenzymes results in a broader range of substrate oxidation capacity.

The kinetic properties and amino acid substitutions within the substrate binding sites of primate ADH isoforms were examined in order to understand how ethanol oxidizing capability has been selected for during primate evolution. Amino acid substitutions of the inner (positions 48 and 93), middle (141, 294, 309, and 318), and outer (57, 116, and 306) regions of the substrate binding pocket were compared and analyzed [Tables 13 & 14]. Ultimately, the different topologies of substrate binding pockets derived from amino acid substitutions were used to explain the substrate preferences of the individual ADH isoforms.

2. ADH Isoenzymes from Marmoset (2M & 10M) and Brown Lemur (4B & 22B)

When comparing kinetic properties among the four primate isoenzymes observed, it appears as though 4B and 2M displayed similar properties; whereas 22B and 10M displayed similar properties [Tables 7-9]. Both isoenzymes 4B and 2M exhibited highest V_{max}/K_m values for ethanol. The catalytic efficiencies change very little for propanol, butanol, pentanol, and hexanol. Furthermore, both 4B and 2M display relatively higher K_m values for cyclohexanol in comparison to 22B and 10M, respectively. Both of these observations are likely due to the presence of threonine at position 48 in these isoenzymes [Figures 14-A & 15-A]. Like with human ββ, the additional methyl group in the threonine side chain interferes with the binding of alcohols with substitutes other than two hydrogens at the C1 position (Niederhut *et al.* 2001). Thus, secondary alcohols are generally poor substrates for isoenzymes containing Thr-48 (Eklund *et al.* 1987).

The primate isoenzymes 22B and 10M both exhibit V_{max}/K_m values that increase with increasing substrate chain length. Furthermore, 22B and 10M also both display lower K_m values for cyclohexanol compared to 4B and 2M, respectively [Tables 7-9]. These observations are probably due to the presence of serine at position 48 in these isoenzymes—which gives a larger space (compared to Thr-48) for bulkier substrates like cyclohexanol [Figures 14-B & 15-B] (Hoog *et al.* 1992). This larger space can also explain the increasing catalytic efficiencies as the substrate chain length increases. In essence, as the size of the substrate increases, the V_{max}/K_m value increases. Thus, it appears as though the longer-chain substrates fill the substrate-binding pocket and interact more favorably with the enzyme (Light *et al.* 1992). In conclusion, long-chain primary alcohols and secondary alcohols like cyclohexanol are fairly good substrates for ADH isoenzymes containing Ser-48—as observed with human γγ.

Although the most substantial changes in substrate specificity result from amino acid substitutions within the inner region of the substrate-binding site (residues 48 and 93), substitutions in the middle and outer regions can also effect substrate specificity (Niederhut *et al.* 2001).

As previously stated, isoenzymes 4B and 2M display similar trends in kinetic properties; however, the V_{max}/K_m value for cyclohexanol is 25-fold higher for 2M compared to 4B [Table 9]. In order to determine where this difference in substrate preference arises, a good starting point would be to determine where 4B and 2M differ in amino acid at positions within the substrate binding site. These isoenzymes differ at residues 318, 57, and 306—where 4B contains Val-318, Met-57, and Leu-306, and 2M contains Leu-318, Leu-57, and Met-306. It can be observed that Leu-318 in 2M is

positioned to yield more room in the substrate binding site than the corresponding Val-318 present in 4B. In addition to this observation, the presence of Leu-57 in 2M also gives more space compared to the larger Met-57 present in 4B [Figures 16-A & 16-B]. The additional space created in 2M at positions 318 and 57 probably explains why cyclohexanol is a better substrate for 2M compared to 4B.

Although the isoenzymes 22B and 10M displayed similar kinetic trends, noticeable differences between the two isoenzymes are: (1) the V_{max}/K_m value for ethanol is 25-fold higher for 10M compared to 22B, and (2) the V_{max}/K_m value for cyclohexanol is 73-fold higher for 10M compared to 22B [Table 9]. These two isoenzymes differ at four residues within the substrate-binding site—141, 57, 116, and 306. It can be observed that 22B contains Ala-141 in the middle region of the substrate binding site, while 10M contains Leu-141. The substitution of Leu→Ala-141 generates more space; which may explain why 10M has a 25-fold higher V_{max}/K_m value for ethanol compared to 22B [Figures 17-A & 17-B]. In addition to position 141, 22B and 10M differ at three positions within the outer region of the substrate binding site—57, 116, and 306. While 22B contains Ile-57, Val-116, and Leu-306, 10M contains Leu-57, Leu-116, and Met-306. The three outer amino acids present in 22B are smaller than all of the amino acids present in 10M (in respective positions). These smaller groups present in 22B yield a larger substrate binding site [Figures 18-A & 18-B]. It is possible that cyclohexanol is a worse substrate for 22B compared to 10M due to the fact that the substrate binding site is too big; thus, cyclohexanol doesn't interact with the isoenzyme as well.

It can be observed that all four primate isoenzymes exhibited the lowest K_m values and the highest V_{max}/K_m values with *trans*-2-hexen-1-ol as a substrate [Tables 7-

9]. This phenomena is probably due to the fact that *trans*-2-hexen-1-ol resembles the alcohol end of retinol—which is an established substrate *in vivo* for alcohol dehydrogenases (Julia *et al.* 1986). The competitive oxidation of ethanol over retinol by alcohol dehydrogenase has been proposed to interfere with retinoic acid synthesis—which can cause fetal alcohol syndrome, or FAS (Duester 1991; Pullarkat 1991).

trans-2-hexen-1-ol

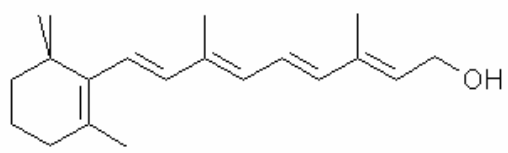

Retinol

The kinetic data obtained from each primate's pair of isoenzymes can be used to predict which species would be better-suited for ethanol oxidation [Tables 7-9]. Since the average V_{max}/K_m value with ethanol for the two isoenzymes from marmoset (29.5 min^{-1} mM^{-1}) is higher than the average calculated from the brown lemur isoenzymes (15.6 $min^{-1}mM^{-1}$), marmoset would appear to have a better capacity for ethanol oxidation. This observation supports the suggestion that ethanol oxidation occurred late in primate evolution since lemurs and humans diverged from a common ancestor 62-65 million years ago, while humans and marmosets diverged 35-40 million years ago (Yoder & Yang 2004; Cronin & Sarich 1978).

3. Ancestral ADH Isoenzymes (Sigma 2-1 & Sigma 2-2)

Kinetic properties and amino acid substitutions within the substrate binding sites of the ancestral ADH isoforms, Sigma 2-1 and Sigma 2-2, were also examined and compared to human σσ-ADH [Tables 10-12; Table 14].

Both ancestral ADH isoforms exhibit catalytic efficiencies that increase with increasing substrate chain length, as well as K_m values that decrease with increasing chain length. Both of these trends are also demonstrated in human σσ; however, K_m values are several-fold lower and V_{max}/K_m values are several-fold higher for σσ compared to Sigma 2-1 and Sigma 2-2. These observations are likely a result of the amino acid substitution at position 294—where σσ contains Val-294, and both ancestral isoforms contain Ala-294 (which is also present in the rat class IV ADH isoenzyme). The exchange of valine to alanine in the middle region of the substrate binding pocket results in extra space at the active site…which explains why Sigma 2-1 and Sigma 2-2 have such a low affinity for small substrates like ethanol [Figures 4-A, 4-B, & 4-C] (Farres *et al.* 1994). This is demonstrated in Table 10, where Sigma 2-1 and Sigma 2-2 display approximate 12-fold increases in K_m values for ethanol compared to σσ.

The change from Ala-294 to Val-294 in primate ADH evolution suggests that a major adaptation to ethanol occurred very recently—based on the drastic shift in K_m for ethanol [Table 10]. It is estimated that this single A294V change occurred between node 34 and modern human about 15 million years ago [Figure 6]; due to the fact that human, chimp, and gorilla all have this A294V change, but orangutan does not (Carrigan 2011).

Although Sigma 2-1 and Sigma 2-2 display very similar kinetic trends, Sigma 2-2 demonstrates an approximate 2-fold decrease in K_m values for substrates longer than propanol, and demonstrates higher catalytic efficiencies for all substrates; ranging from 1.3-fold to 6-fold increases [Tables 10-12]. These differences probably arise from the amino acid substitution of Val-116 for Ile-116 in Sigma 2-2 [Table 14]. Since the isoleucine residue is larger than valine, it provides a better contact surface for longer

chain alcohol substrates which explains the lower K_m values of Sigma 2-2 with butanol, pentanol, and hexanol [Figures 4-B & 4-C] (Hoog *et al.* 1992).

Similar to the primate isoenzymes, Sigma 2-1 and Sigma 2-2 displayed lowest K_m values and highest V_{max}/K_m values with *trans*-2-hexen-1-ol as a substrate [Tables 10-12]. Furthermore, Sigma 2-1 demonstrated catalytic efficiencies that were 13-17-fold higher than the primate isoenzymes with *trans*-2-hexen-1-ol, and Sigma 2-2 exhibited values that were 33-46-fold higher than primate isoenzymes. This observation correlates to the finding that human σσ isoenzymes are more efficient at oxidizing retinol than any other human isoenzyme (Yang *et al.* 1994).

4. Summary of Findings

The kinetic data obtained from the primate Class I ADH experiments indicates that the common marmoset has a higher catalytic efficiency towards ethanol oxidation than the brown lemur—due to the fact that the average catalytic efficiency calculated for the two isoforms from marmoset was approximately 2-fold higher than the average calculated for the two isoforms from brown lemur. This finding supports the hypothesis that the species with the higher content of fermentable fruit in its diet has a higher catalytic efficiency towards ethanol oxidation—since marmosets display a preference for fruit when it is available, while brown lemurs have access to fruits year-round but are classified as opportunistic foragers.

The kinetic data obtained from the human ancestral Class IV ADH experiments indicates that the single A294V change, which occurred approximately 15 million years ago in primate evolution, increased the catalytic efficiency of this isoenzyme towards ethanol oxidation by approximately 80-fold. This finding supports the hypothesis that the

ability of Class IV ADH to efficiently oxidize ethanol developed late in primate evolution and results primarily from the singe A294V change. A likely explanation for this change is that a higher catalytic efficiency toward ethanol in the Class IV ADH isoenzyme permits greater ethanol oxidizing capacity during first-pass metabolism and thus allows the organism to handle greater dietary loads of ethanol without functional impairment.

Table 13: Amino Acids Present in the Substrate Site of ADHs from Marmoset and Brown Lemur

REGION	Position	Human Class I			Brown Lemur		Marmaset	
		αα	ββ	γγ	4B	22B	2M	10M
INNER	48	Thr	Thr	Ser	Thr	Ser	Thr	Ser
	93	Ala	Phe	Phe	Phe	Phe	Phe	Phe
MIDDLE	141	Leu	Leu	Val	Leu	Ala	Leu	Leu
	294	Val	Val	Val	Val	Val	Val	Val
	309	Leu	Leu	Leu	Leu	Leu	Leu	Leu
	318	Ile	Val	Ile	Val	Val	Leu	Val
OUTER	57	Met	Leu	Leu	Met	Ile	Leu	Leu
	116	Val	Leu	Leu	Leu	Val	Leu	Leu
	306	Met	Met	Met	Leu	Leu	Met	Met

Table 14: Amino Acids Present in the Substrate Site of Ancestral ADHs and Human σσ-ADH

REGION	Position	Human Class IV	Human Ancestral	
		σσ	Sigma2-1	Sigma2-2
INNER	48	Thr	Thr	**Ser**
	93	Phe	Phe	Phe
MIDDLE	141	Met	Met	Met
	294	Val	**Ala**	**Ala**
	309	Phe	Phe	Phe
	318	Val	Val	Val
OUTER	57	Met	Met	Met
	116	Ile	**Val**	Ile
	306	Met	Met	Met

Figure 4: Comparison of Substrate Sites from Ancestral ADH isoenzymes with Human σσ-ADH

A. Human σσ-ADH Substrate Site

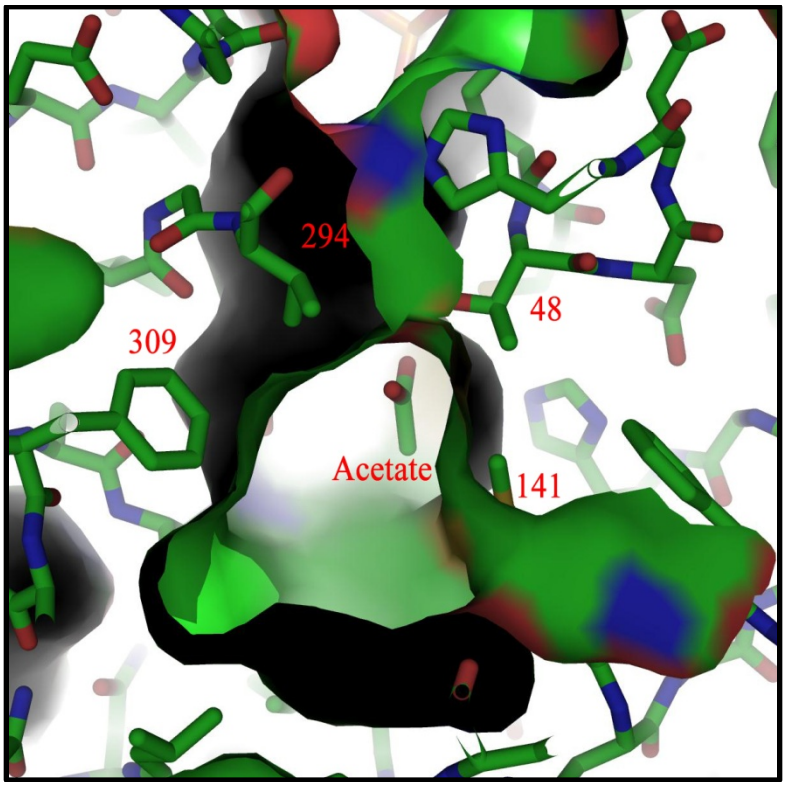

Figure 4-A

-Human σσ-ADH substrate site displaying Thr-48 in the Inner Region, and Met-141, Val-294, and Phe-309 in the Middle Region of the substrate binding site.
-Generated with PyMOL.

B. Ancestral, Sigma 2-1 ADH Substrate Site

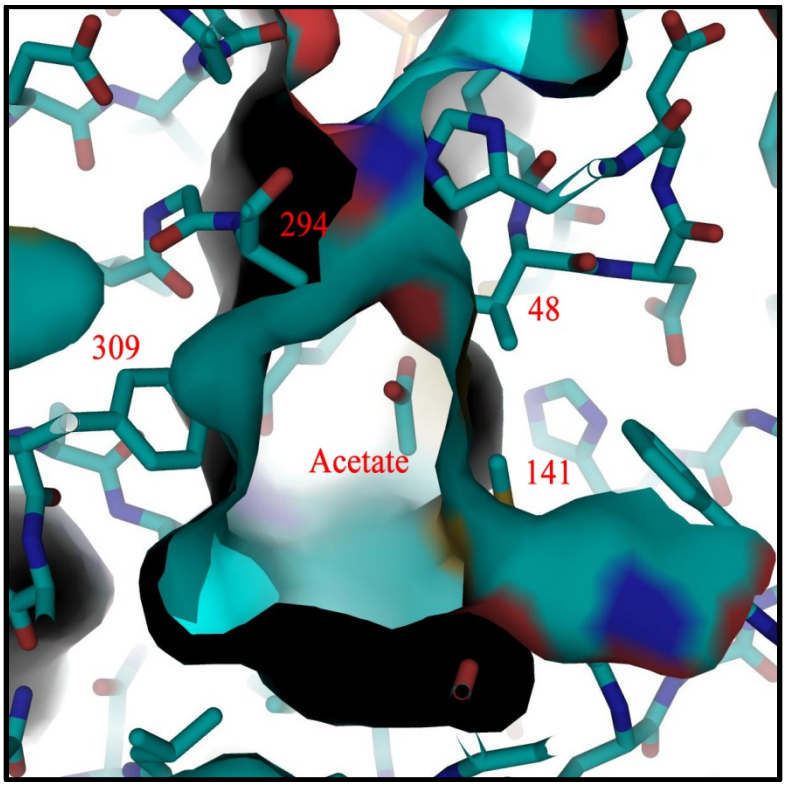

Figure 4-B

-Sigma 2-1 ADH substrate site displaying Thr-48 in the Inner Region, and Met-141, Ala-294, and Phe-309 in the Middle Region of the substrate binding site.
-The Val→Ala substitution at position 294 creates extra space at the active site.
-Generated with PyMOL.

Figure 4: Comparison of Substrate Sites from Ancestral ADH Isoenzymes with Human σσ-ADH (continued)

C. Ancestral, Sigma 2-2 ADH Substrate Site

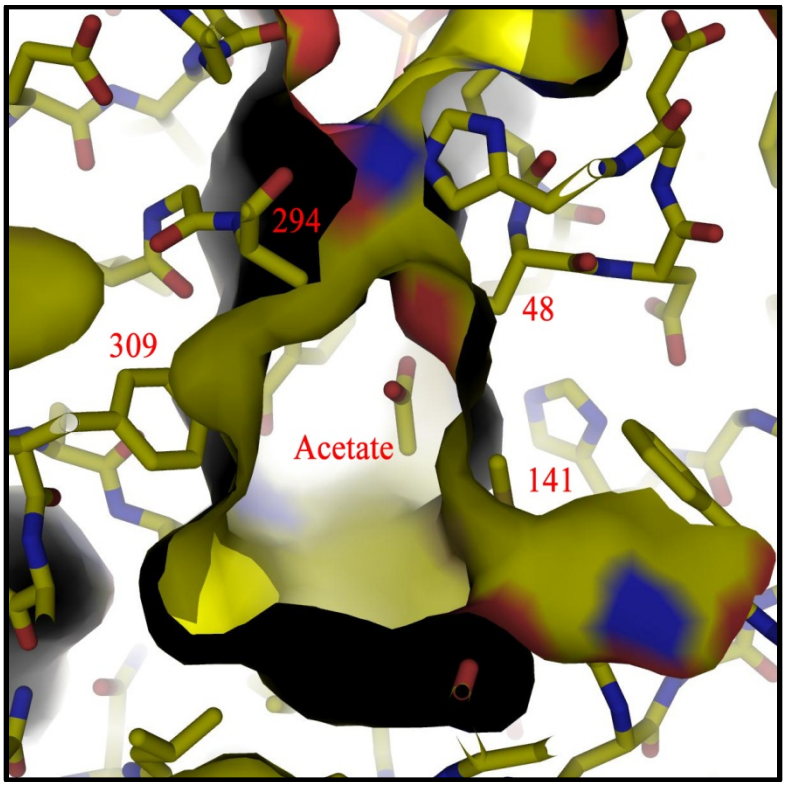

Figure 4-C

-Sigma 2-2 ADH substrate site displaying Ser-48 in the Inner Region, and Met-141, Ala-294, and Phe-309 in the Middle Region of the substrate binding site.
-The Thr→Ser substitution at position 48 creates extra space at the active site when compared to that of Sigma 2-1.
-Generated with PyMOL.

Figure 14: Comparison of Position 48 in the Substrate Sites of4B and 22B from Brown Lemur

A. 4B-ADH Substrate Site Displaying Position 48

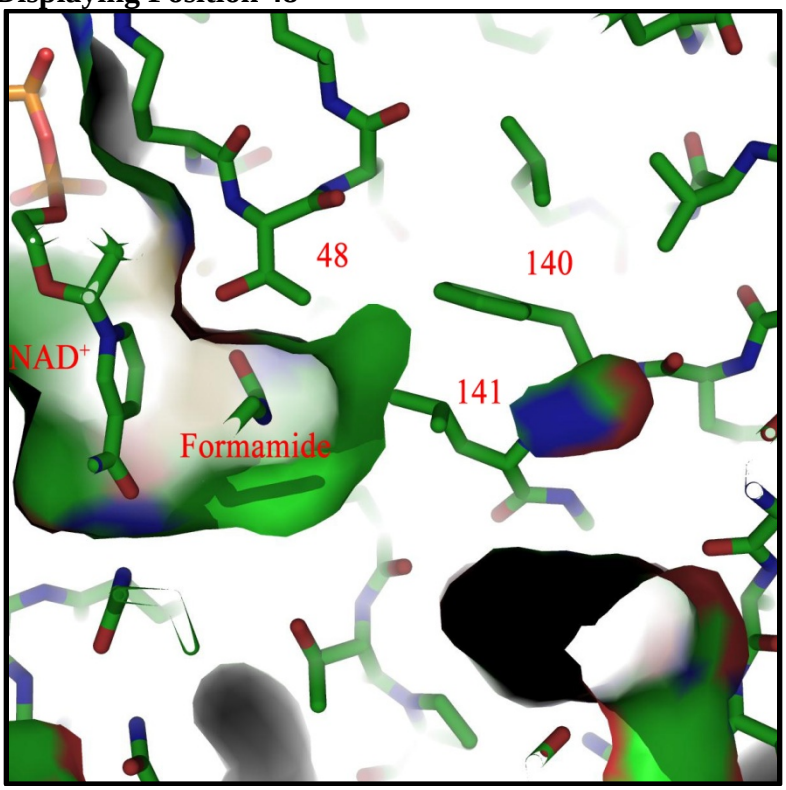

Figure 14-A

-4B-ADH substrate site displaying Thr-48 in the Inner Region, in addition to Phe-140 and Leu-141 in the Middle Region of the substrate binding site.
-Generated with PyMOL.

B. 22B-ADH Substrate Site Displaying Position 48

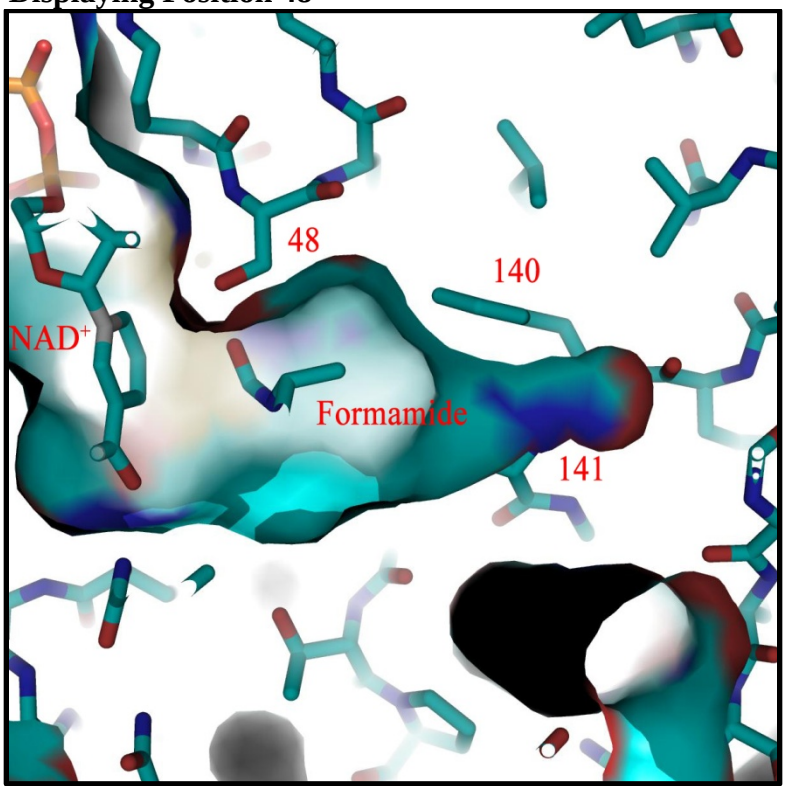

Figure 14-B

-22B-ADH substrate site displaying Ser-48 in the Inner Region, in addition to Phe-140 and Ala-141 in the Middle Region of the substrate binding site.
-The Thr→Ser substitution at position 48 creates extra space at the active site in comparison to 4B.
-Generated with PyMOL.

Figure 15: Comparison of Position 48 in the Substrate Sites of 2M and 10M from Marmoset

A. 2M-ADH Substrate Site Displaying Position 48

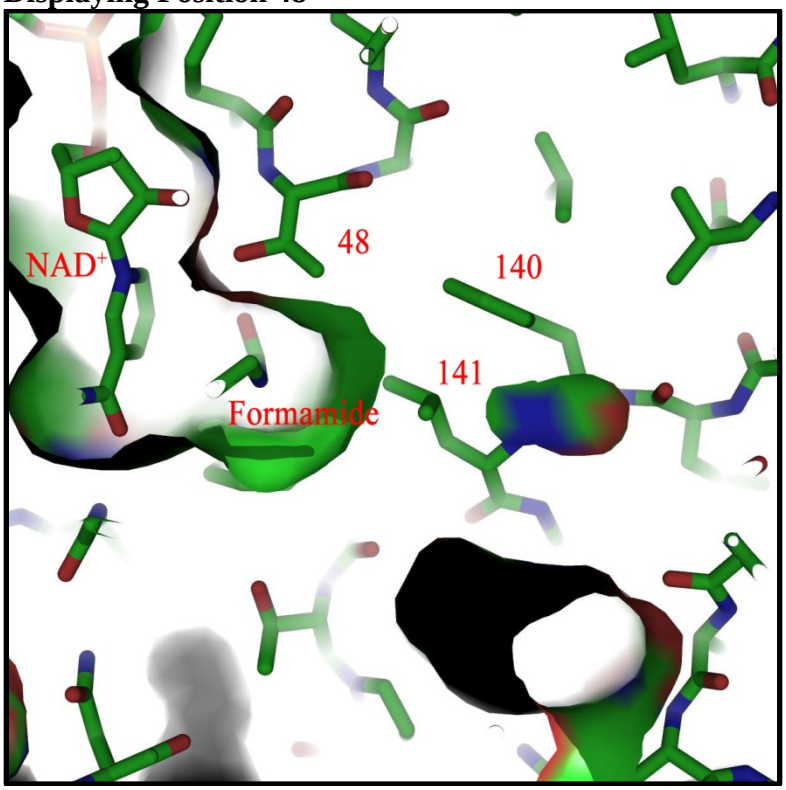

Figure 15-A

-2M-ADH substrate site displaying Thr-48 in the Inner Region, as well as Phe-140 and Leu-141 in the Middle Region of the substrate binding site.
-Generated with PyMOL.

B. 10M-ADH Substrate Site Displaying Position 48

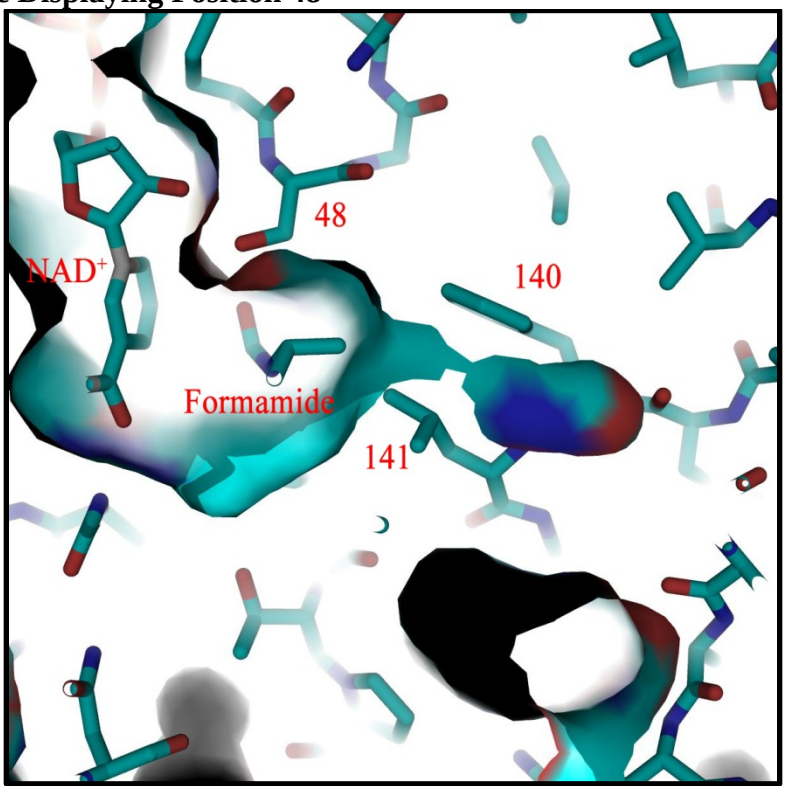

Figure 15-B

-10M-ADH substrate site displaying Ser-48 in the Inner Region, in addition to Phe-140 and Leu-141 in the Middle Region of the substrate binding site.
-The Thr→Ser substitution at position 48 creates extra space at the active site in comparison to 2M.
-Generated with PyMOL.

Figure 16: Comparison of Substrate Sites of 4B from Brown Lemur and 2M from Marmoset

A. 4B-ADH Substrate Site

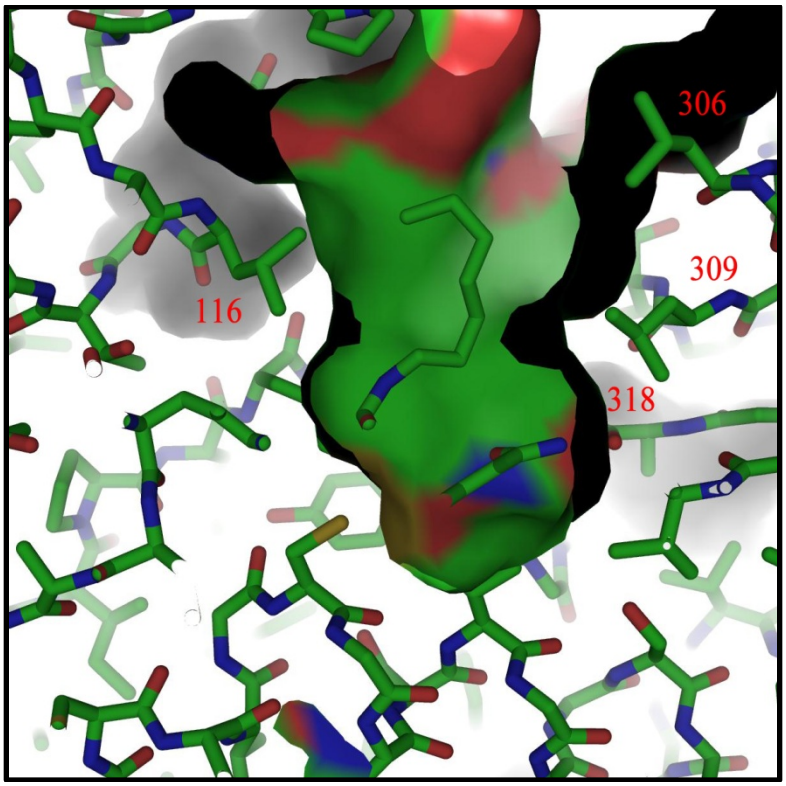

Figure 16-A

-4B-ADH substrate site displaying Leu-309 and Val-318 in the Middle Region, as well as Leu-116 and Leu-306 in the Outer Region of the substrate binding site.
-Generated with PyMOL.

B. 2M-ADH Substrate Site

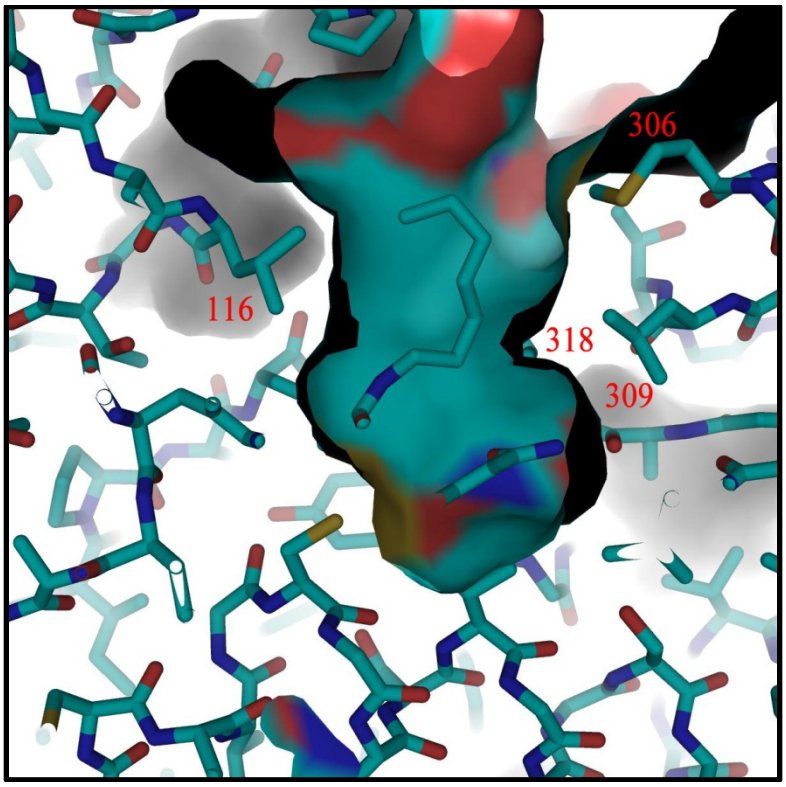

Figure 16-B

-2M-ADH substrate site displaying Leu-309 and Leu-318 in the Middle Region, as well as Leu-116 and Met-306 in the Outer Region of the substrate binding site.
-Both exchanges, Val→Leu at position 318 and Met-Leu at position 57, result in extra space in the substrate site.
-Generated with PyMOL.

Figure 17: Comparison of Position 141 in the substrate sites of 22B from Brown Lemur and 10M from Marmoset

A. 22B-ADH Substrate Site

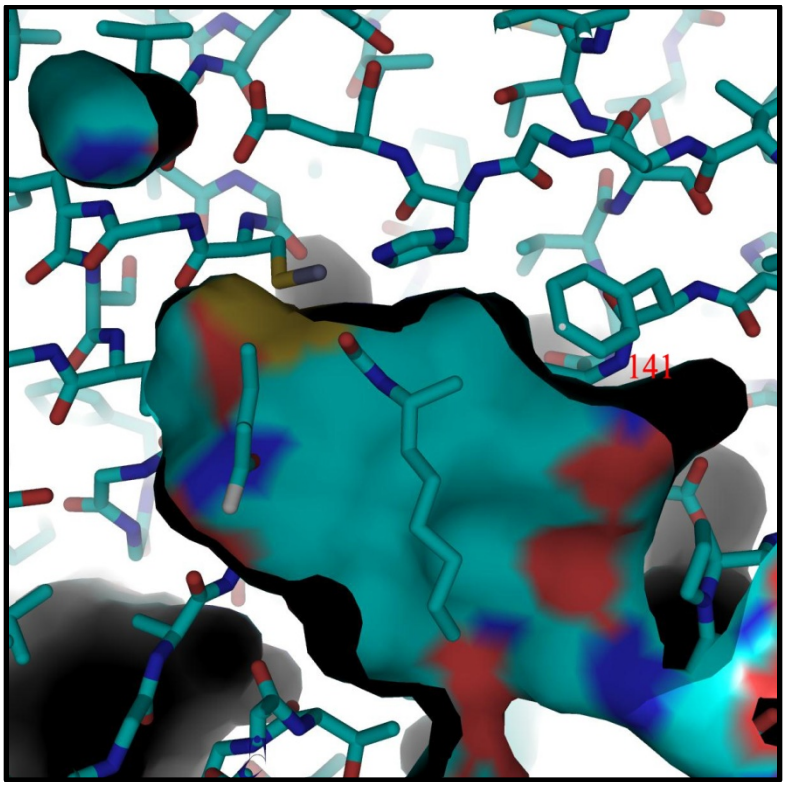

Figure 17-A

-22B-ADH substrate site displaying Ala-141 in the Middle Region, of the substrate binding site.
-Generated with PyMOL.

B. 10M-ADH Substrate Site

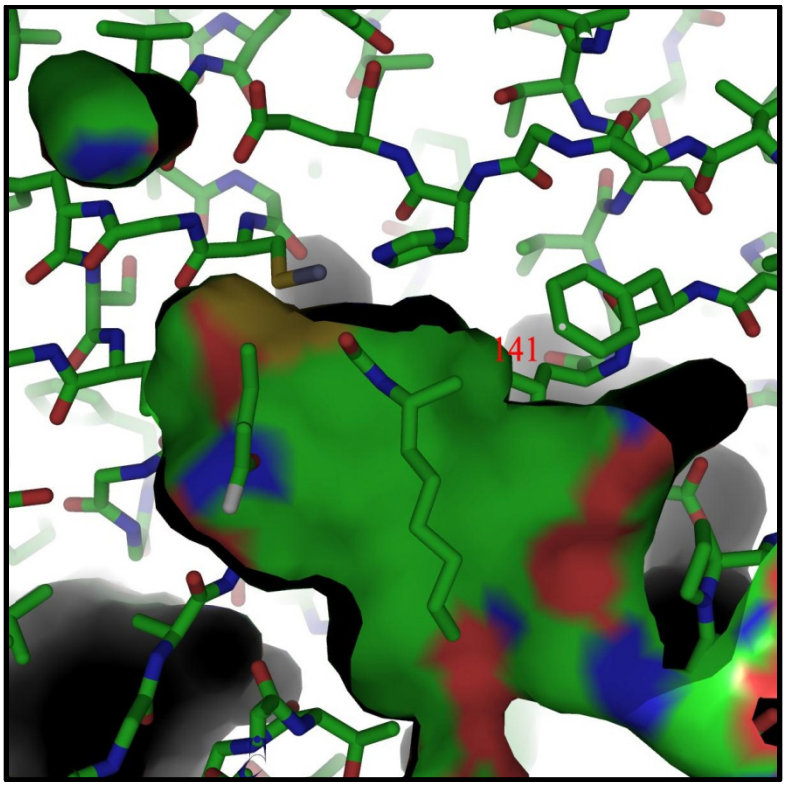

Figure 17-B

-10M-ADH substrate site displaying Leu-141 in the Middle Region, of the substrate binding site.
-The Ala→Leu substitution at position 141 leaves less space in the substrate binding site compared to 22B.
-Generated with PyMOL.

Figure 18: Comparison of Positions 57 and 116 in the Substrate Sites of 22B from Brown Lemur and 10M from Marmoset

A. 22B-ADH Substrate Site

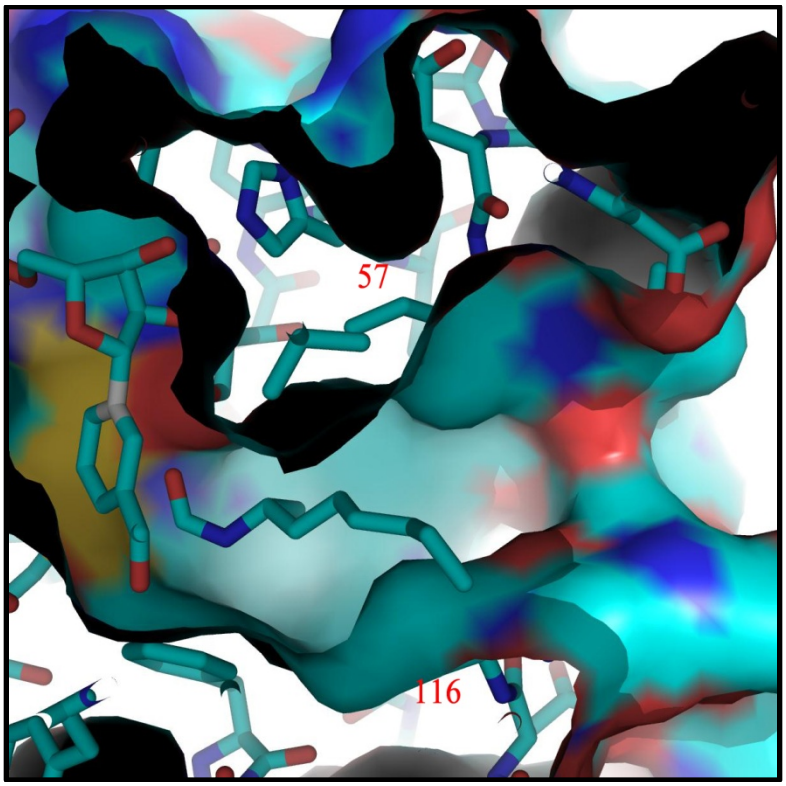

Figure 18-A

-22B-ADH substrate site displaying Ile-57 and Val-116 in the Outer Region of the substrate binding site.
-Generated with PyMOL.

B. 10M-ADH Substrate Site

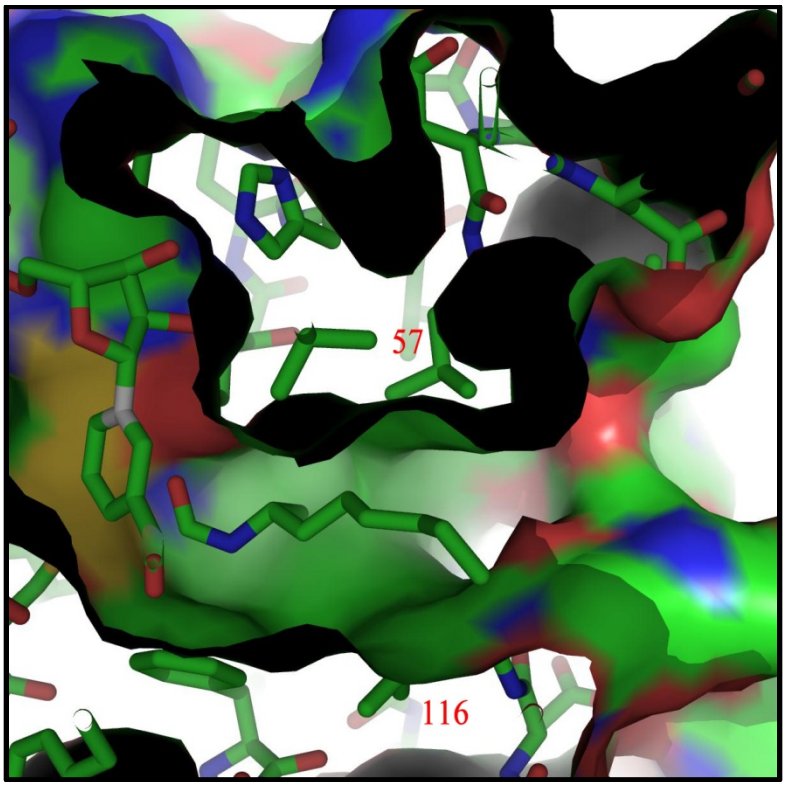

Figure 18-B

-10M-ADH substrate site displaying Leu-57 and Leu-116 in the Outer Region of the substrate binding site.
-Both, the Ile→Leu substitution at position 57 and the Val→Leu substitution at position yield less room in the substrate binding site compared to 22B.
-Generated with PyMOL.

V. CONCLUSIONS

Data obtained from experiments with both, Class I and Class IV ADH isoenzymes supports the proposal that recent events occurred during primate evolution that increased the capacity to efficiently oxidize ethanol. Two main conclusions can be drawn with respect to the evolution of ethanol metabolism in primates: (1) multiple Class I ADH duplication events occurred during primate evolution which resulted in a broader substrate-oxidizing capacity. This discovery supports the suggestion that primate Class I ADH evolution is associated with dietary adaptations in the primate lineage. (2) A separate event, consisting of a single amino acid exchange, occurred 15 million years ago which resulted in a 79-fold increase in the ethanol-oxidizing capability of Class IV ADH isoenzymes.

REFERENCES

Beier, J. I. & Arteel, G. E. (2012). Alcoholic liver disease and the potential role of plasminogen activator inhibitor-1 and fibrin metabolism. *Exp Biol Med (Maywood)* **237**, 1-9.

Blacklin, C. I. (1958). The equilibrium constant of the system ethanol, aldehyde, dpn, dpnh and h. *Acta Chem Scand* **12**, 7.

Bosron, W. F., Li, T. K., Dafeldecker, W. P. & Vallee, B. L. (1979). Human liver pi-alcohol dehydrogenase: Kinetic and molecular properties. *Biochemistry* **18**, 1101-5.

Branden, C. I., Jornvall, H., Eklund, H. & Furugren, B. (1975). Alcohol dehydrogenases. *The Enzymes* **11**, 86.

Carrigan, M. (2011). (Hurley, T. D., ed.), pp. 3.

Carrigan, M. A., Uryasev, O. S., Hurley, T. D., Zhai, L., Myers, C., Davis, R. W. & Benner, S. A. (2012). Gene conversion and the natural history of class i primate alcohol dehydrogenases pp. 35. Foundation for Applied Molecular Evolution; Department of Biochemistry and Molecular Biology, Indiana University School of Medicine, Gainesville, FL;
Indianapolis, IN.

Caton, J. M., Hill, D. M., Hume, I. D. & Crook, G. A. (1996). The digestive strategy of the common marmoset, callithrix jacchus. *Comp Biochem Physiol A Physiol* **114**, 1-8.

Coimbra Filho, A. F. & Mittermeier, R. A. (1978). Tree-gouging, exudate-eating and the "short-tusked" condition in callithrix and cebuella. *The biology and conservation of the callitrichidae,* 10.

Crabb, D. W., Bosron, W. F. & Li, T. K. (1983). Steady-state kinetic properties of purified rat liver alcohol dehydrogenase: Application to predicting alcohol elimination rates in vivo. *Arch Biochem Biophys* **224**, 299-309.

Cronin, J. E. & Sarich, V. M. (1978). Marmoset evolution: The molecular evidence. *Primates Med* **10**, 12-9.

Crow, K. E. & Hardman, M. J. (1989). Regulations of rates of ethanol metabolism. *Human metabolism of alcohol* **2**, 14.

Dellarco, V. L. (1988). A mutagenicity assessment of acetaldehyde. *Mutat Res* **195**, 1-20.

Deltour, L., Foglio, M. H. & Duester, G. (1999). Metabolic deficiencies in alcohol dehydrogenase adh1, adh3, and adh4 null mutant mice. Overlapping roles of adh1 and adh4 in ethanol clearance and metabolism of retinol to retinoic acid. *J Biol Chem* **274**, 16796-801.

Dudley, R. (2004). Ethanol, fruit ripening, and the historical origins of human alcoholism in primate frugivory. *Integr Comp Biol* **44**, 315-23.

Duester, G. (1991). A hypothetical mechanism for fetal alcohol syndrome involving ethanol inhibition of retinoic acid synthesis at the alcohol dehydrogenase step. *Alcohol Clin Exp Res* **15**, 568-72.

Duester, G., Farres, J., Felder, M. R., Holmes, R. S., Hoog, J. O., Pares, X., Plapp, B. V., Yin, S. J. & Jornvall, H. (1999). Recommended nomenclature for the vertebrate alcohol dehydrogenase gene family. *Biochem Pharmacol* **58**, 389-95.

Eaton, S. B., Eaton, S. B., 3rd & Konner, M. J. (1997). Paleolithic nutrition revisited: A twelve-year retrospective on its nature and implications. *Eur J Clin Nutr* **51**, 207-16.

Edenberg, H. & Bosron, W. F. (1997). Alcohol dehydrogenases. *Comprehensive Toxicology* **3**.

Edenberg, H. J. (2000). Regulation of the mammalian alcohol dehydrogenase genes. *Prog Nucleic Acid Res Mol Biol* **64**, 295-341.

Eklund, H., Horjales, E., Vallee, B. L. & Jornvall, H. (1987). Computer-graphics interpretations of residue exchanges between the alpha, beta and gamma subunits of human-liver alcohol dehydrogenase class i isozymes. *Eur J Biochem* **167**, 185-93.

Eklund, H., Muller-Wille, P., Horjales, E., Futer, O., Holmquist, B., Vallee, B. L., Hoog, J. O., Kaiser, R. & Jornvall, H. (1990). Comparison of three classes of human liver alcohol dehydrogenase. Emphasis on different substrate binding pockets. *Eur J Biochem* **193**, 303-10.

Eklund, H., Nordstrom, B., Zeppezauer, E., Soderlund, G., Ohlsson, I., Boiwe, T., Soderberg, B. O., Tapia, O., Branden, C. I. & Akeson, A. (1976). Three-dimensional structure of horse liver alcohol dehydrogenase at 2-4 a resolution. *J Mol Biol* **102**, 27-59.

Ewing, J. A. (1984). Detecting alcoholism. The cage questionnaire. *JAMA* **252**, 1905-7.

Farres, J., Moreno, A., Crosas, B., Peralba, J. M., Allali-Hassani, A., Hjelmqvist, L., Jornvall, H. & Pares, X. (1994). Alcohol dehydrogenase of class iv (sigma sigma-adh) from human stomach. Cdna sequence and structure/function relationships. *Eur J Biochem* **224**, 549-57.

Ferrari, S. F. & Lopes Ferrari, M. A. (1989). A re-evaluation of the social organisation of the callitrichidae, with reference to the ecological differences between genera. *Folia Primatol (Basel)* **52**, 132-47.

Flotte, T. R., Fischer, A. C., Goetzmann, J., Mueller, C., Cebotaru, L., Yan, Z., Wang, L., Wilson, J. M., Guggino, W. B. & Engelhardt, J. F. (2010). Dual reporter comparative indexing of raav pseudotyped vectors in chimpanzee airway. *Mol Ther* **18**, 594-600.

Friedman, S. L. (2008). Mechanisms of hepatic fibrogenesis. *Gastroenterology* **134**, 1655-69.

Garber, P. A. (1992). Vertical clinging, small body size, and the evolution of feeding adaptations in the callitrichinae. *Am J Phys Anthropol* **88**, 469-82.

Gaulin, S. J. C. & Konner, M. (1977). On the natural diet of primates, including humans. *Nutrition and the brain* **1**, 86.

Gibbons, B. J. & Hurley, T. D. (2004). Structure of three class i human alcohol dehydrogenases complexed with isoenzyme specific formamide inhibitors. *Biochemistry* **43**, 12555-62.

Gingerich, P. D. & Uhen, M. D. (1994). Time of origin of primates. *Journal of Human Evolution* **27**, 3.

Grine, F. E. & Kay, R. F. (1988). Early hominid diets from quantitative image analysis of dental microwear. *Nature* **333**, 765-8.
Hill, D. B. & Kugelmas, M. (1998). Alcoholic liver disease. Treatment strategies for the potentially reversible stages. *Postgrad Med* **103**, 261-4, 7-8, 73-5.
Holmquist, B. & Vallee, B. L. (1991). Human liver class iii alcohol and glutathione dependent formaldehyde dehydrogenase are the same enzyme. *Biochem Biophys Res Commun* **178**, 1371-7.
Hoog, J. O., Eklund, H. & Jornvall, H. (1992). A single-residue exchange gives human recombinant beta beta alcohol dehydrogenase gamma gamma isozyme properties. *Eur J Biochem* **205**, 519-26.
Hoog, J. O. & Ostberg, L. J. (2011). Mammalian alcohol dehydrogenases--a comparative investigation at gene and protein levels. *Chem Biol Interact* **191**, 2-7.
Hur, M. W. & Edenberg, H. J. (1995). Cell-specific function of cis-acting elements in the regulation of human alcohol dehydrogenase 5 gene expression and effect of the 5'-nontranslated region. *J Biol Chem* **270**, 9002-9.
Hurley, T. D. & Bosron, W. F. (1992). Human alcohol dehydrogenase: Dependence of secondary alcohol oxidation on the amino acids at positions 93 and 94. *Biochem Biophys Res Commun* **183**, 93-9.
Hurley, T. D., Edenberg, H. & Li, T. K. (2002). Pharmacogenomics of alcoholism. *Pharmacogenomics: The Search for Individualized Therapies*.
Inatomi, N., Kato, S., Ito, D. & Lieber, C. S. (1989). Role of peroxisomal fatty acid beta-oxidation in ethanol metabolism. *Biochem Biophys Res Commun* **163**, 418-23.
Julia, P., Farres, J. & Pares, X. (1986). Ocular alcohol dehydrogenase in the rat: Regional distribution and kinetics of the adh-1 isoenzyme with retinol and retinal. *Exp Eye Res* **42**, 305-14.
Kedishvili, N. Y., Bosron, W. F., Stone, C. L., Hurley, T. D., Peggs, C. F., Thomasson, H. R., Popov, K. M., Carr, L. G., Edenberg, H. J. & Li, T. K. (1995). Expression and kinetic characterization of recombinant human stomach alcohol dehydrogenase. Active-site amino acid sequence explains substrate specificity compared with liver isozymes. *J Biol Chem* **270**, 3625-30.
Kim, W. R., Brown, R. S., Jr., Terrault, N. A. & El-Serag, H. (2002). Burden of liver disease in the united states: Summary of a workshop. *Hepatology* **36**, 227-42.
Klopfer, P. H. (1970). Discrimination of young in galagos. *Folia Primatol (Basel)* **13**, 137-43.
Klopfer, P. H. & Jolly, A. (1970). The stability of territorial boundaries in a lemur troop. *Folia Primatol (Basel)* **12**, 199-208.
Koivusalo, M., Baumann, M. & Uotila, L. (1989). Evidence for the identity of glutathione-dependent formaldehyde dehydrogenase and class iii alcohol dehydrogenase. *FEBS Lett* **257**, 105-9.
Lands, W. E. (1998). A review of alcohol clearance in humans. *Alcohol* **15**, 147-60.
Li, T. K. (2000). Pharmacogenetics of responses to alcohol and genes that influence alcohol drinking. *J Stud Alcohol* **61**, 5-12.
Lieber, C. S. (1991). Hepatic, metabolic and toxic effects of ethanol: 1991 update. *Alcohol Clin Exp Res* **15**, 573-92.

Light, D. R., Dennis, M. S., Forsythe, I. J., Liu, C. C., Green, D. W., Kratzer, D. A. & Plapp, B. V. (1992). Alpha-isoenzyme of alcohol dehydrogenase from monkey liver. Cloning, expression, mechanism, coenzyme, and substrate specificity. *J Biol Chem* **267**, 12592-9.

Martin, R. D. (1993). Primate origins: Plugging the gaps. *Nature* **363**, 223-34.

Milton, K. (1999). Nutritional characteristics of wild primate foods: Do the diets of our closest living relatives have lessons for us? *Nutrition* **15**, 488-98.

Moran, L. A., Scrimgeour, K. G., Horton, H. R., Ochs, R. S. & Rawn, J. D. (1994). *Biochemistry*, Prentice Hall, Englewood Cliffs, NJ.

Niederhut, M. S., Gibbons, B. J., Perez-Miller, S. & Hurley, T. D. (2001). Three-dimensional structures of the three human class i alcohol dehydrogenases. *Protein Sci* **10**, 697-706.

Olshan, A. F., Weissler, M. C., Watson, M. A. & Bell, D. A. (2001). Risk of head and neck cancer and the alcohol dehydrogenase 3 genotype. *Carcinogenesis* **22**, 57-61.

Oota, H., Dunn, C. W., Speed, W. C., Pakstis, A. J., Palmatier, M. A., Kidd, J. R. & Kidd, K. K. (2007). Conservative evolution in duplicated genes of the primate class i adh cluster. *Gene* **392**, 64-76.

Pullarkat, R. K. (1991). Hypothesis: Prenatal ethanol-induced birth defects and retinoic acid. *Alcohol Clin Exp Res* **15**, 565-7.

Radosavljevic, T., Mladenovic, D. & Vucevic, D. (2009). [the role of oxidative stress in alcoholic liver injury]. *Med Pregl* **62**, 547-53.

Ramaiah, S., Rivera, C. & Arteel, G. (2004). Early-phase alcoholic liver disease: An update on animal models, pathology, and pathogenesis. *Int J Toxicol* **23**, 217-31.

Rylands, A. B. (1984). Tree-gouging and exudate feeding in marmosets (callitrichidae, primates). *Tropical rain forest: the leeds symposium*, 13.

Schuppan, D., Ruehl, M., Somasundaram, R. & Hahn, E. G. (2001). Matrix as a modulator of hepatic fibrogenesis. *Semin Liver Dis* **21**, 351-72.

Shahin, M., Schuppan, D., Waldherr, R., Risteli, J., Risteli, L., Savolainen, E. R., Oesterling, C., Abdel Rahman, H. M., el Sahly, A. M., Abdel Razek, S. M. & et al. (1992). Serum procollagen peptides and collagen type vi for the assessment of activity and degree of hepatic fibrosis in schistosomiasis and alcoholic liver disease. *Hepatology* **15**, 637-44.

Sicard, D. & Legras, J. L. (2011). Bread, beer and wine: Yeast domestication in the saccharomyces sensu stricto complex. *C R Biol* **334**, 229-36.

Smith, M., Hopkinson, D. A. & Harris, H. (1971). Developmental changes and polymorphism in human alcohol dehydrogenase. *Ann Hum Genet* **34**, 251-71.

Smith, M., Hopkinson, D. A. & Harris, H. (1972). Alcohol dehydrogenase isozymes in adult human stomach and liver: Evidence for activity of the adh 3 locus. *Ann Hum Genet* **35**, 243-53.

Sponheimer, M. & Lee-Thorp, J. A. (1999). Isotopic evidence for the diet of an early hominid, australopithecus africanus. *Science* **283**, 368-70.

Stone, C. L., Li, T. K. & Bosron, W. F. (1989). Stereospecific oxidation of secondary alcohols by human alcohol dehydrogenases. *J Biol Chem* **264**, 11112-6.

Stratton, K., Howe, C. & Battaglia, F. (1996). *Fetal alcohol syndrome: Diagnosis, epidemiology, prevention and treatment.*, National Academy Press, Washington, D.C.

Sun, H. W. & Plapp, B. V. (1992). Progressive sequence alignment and molecular evolution of the zn-containing alcohol dehydrogenase family. *J Mol Evol* **34**, 522-35.

Tarnaud, L. (2004). Ontogeny of feeding behavior of *eulemur fulvus* in the dry forest of mayotte. *Int J Primatol* **25**, 21.

Tavare, S., Marshall, C. R., Will, O., Soligo, C. & Martin, R. D. (2002). Using the fossil record to estimate the age of the last common ancestor of extant primates. *Nature* **416**, 726-9.

Wagner, F. W., Pares, X., Holmquist, B. & Vallee, B. L. (1984). Physical and enzymatic properties of a class iii isozyme of human liver alcohol dehydrogenase: Chi-adh. *Biochemistry* **23**, 2193-9.

Xie, P. T. & Hurley, T. D. (1999). Methionine-141 directly influences the binding of 4-methylpyrazole in human sigma sigma alcohol dehydrogenase. *Protein Sci* **8**, 2639-44.

Yang, Z. N., Davis, G. J., Hurley, T. D., Stone, C. L., Li, T. K. & Bosron, W. F. (1994). Catalytic efficiency of human alcohol dehydrogenases for retinol oxidation and retinal reduction. *Alcohol Clin Exp Res* **18**, 587-91.

Yoder, A. D. & Yang, Z. (2004). Divergence dates for malagasy lemurs estimated from multiple gene loci: Geological and evolutionary context. *Mol Ecol* **13**, 757-73.

Yokoyama, A., Muramatsu, T., Ohmori, T., Yokoyama, T., Okuyama, K., Takahashi, H., Hasegawa, Y., Higuchi, S., Maruyama, K., Shirakura, K. & Ishii, H. (1998). Alcohol-related cancers and aldehyde dehydrogenase-2 in japanese alcoholics. *Carcinogenesis* **19**, 1383-7.

CURRICULUM VITAE

Candace R. Myers

Education:

Master of Science in Biotechnology, Indiana University (May 2012)
Indianapolis, IN (IUPUI)
GPA: 3.5

Master's Certificate in Biotechnology, Indiana University (December 2009)
Indianapolis, IN (IUPUI)
GPA: 3.3

Bachelor of Science in Biology/Minor in Chemistry, Indiana University (May 2005)
Bloomington, IN
GPA: 3.4

Research Experience:

Indiana University—Department of Biochemistry and Molecular Biology (January 2010-May 2012
Graduate Student, Dr. Thomas D. Hurley Lab

- Experiments were performed that utilized enzyme kinetic assays with a spectrophotometer; data obtained from these experiments was then analyzed with software programs to obtain kinetic constants for respective isoenzymes.
- Enzyme structures were created and further analyzed with software modeling programs.
- Research focused on specific alcohol dehydrogenase (ADH) isoenzymes from primates in addition to ADH isoenzymes resurrected from human ancestors to determine the similarities and differences in substrate specificities among respective isoenzymes in order to ultimately determine when and why these ADH isoenzymes diverged during human evolution.

Professional Experience:

City of Greenwood—Finance Department (January 2012-present)
Greenwood, IN
Payroll Clerk/Bookkeeper/Accounts Receivable Clerk

- Responsible for processing payroll for all City employees on a bi-weekly basis to ensure the precise and timely distribution of wages to employees.
- Responsible for receipting money from all departments within the City, performing bank/account transfers, preparing and maintaining budgets by department, creating purchase orders, issuing checks to City vendors, and maintaining records for the Board of Aviation Commissioners (B.O.A.C.).
- Responsible for invoicing, receipting, posting payments, and maintaining all accounts for hangar/land-lease tenants at the Greenwood Municipal Airport.

City of Greenwood—Clerk Treasurer's Office (August 2008-December 2011)
Greenwood, IN
Bookkeeper/Accounts Receivable Clerk/Secretary

- Responsible for receipting all Departmental money, creating purchase orders, issuing checks to City vendors, and mailing monthly hangar invoices.
- Responsible for issuing licenses and permits, maintaining records and account balances for ordinance violation citations, directing incoming calls, and handling requests from the public.

Covance C.L.S.—Genomics Department (June 2006-June 2008)
Indianapolis, IN
DNA/RNA Laboratory Technician

- Responsible for the extraction of DNA/RNA from whole (human) blood samples of patients in various clinical trials by utilizing the following extraction methods: automated extraction using a Qiagen® Autopure® (DNA), and manual extraction using Qiagen® manual kits (DNA), Qiagen® PAXgene® kits (RNA), and Versagene™ Tempus® kits (RNA).
- Utilized a 96-well plate spectrophotometer to determine DNA/RNA quality via analysis of nucleic acid concentration and purity (calculated with A_{260}/A_{280} from spectrophotometer results).
- Responsible for diluting DNA/RNA extractions; followed by proper aliquotting and sample storage.
- Other regular duties included problem solving/resolution of various sample inquiries, inventory checks, archiving reports, performing validation tests, follow-ups on pending samples, building samples to loads, verifying patient IDs on sample tubes, performing regular maintenance on instruments, and decontaminating instruments and work area.

Covance C.L.S.—Hematology Department (October 2005-June 2006)
Indianapolis, IN
Laboratory Assistant

- Responsible for the start-up, running, trouble-shooting, and maintenance of Advia® 120s.
- Responsible for pre-reviewing data results from machines and flagging out-of-range blood cell count values.
- Utilized the BioLink® quality control software on a daily basis for purposes of checking controls and R&D values on machines—in order to comply with appropriate audit trails.